HHS Public Access

Author manuscript

Nature. Author manuscript; available in PMC 2017 February 08.

Published in final edited form as:

Nature. 2016 September 08; 537(7619): 234–238. doi:10.1038/nature19334.

Germinal Center hypoxia and regulation of antibody qualities by a hypoxia response system

Sung Hoon Cho[1], **Ariel L. Raybuck**[1], **Kristy Stengel**[2,*], **Mei Wei**[1,*], **Thomas C. Beck**[1], **Emmanuel Volanakis**[3], **James W. Thomas**[1,4], **Scott Hiebert**[2,5,7], **Volker H. Haase**[4,5], and **Mark R. Boothby**[1,4,5,6]

[1]Pathology-Microbiology-Immunology Department, Vanderbilt University, Nashville, TN

[2]Biochemistry Department, Vanderbilt University, Nashville, TN

[3]Pediatrics Department, Vanderbilt University, Nashville, TN

[4]Medicine Department, Vanderbilt University, Nashville, TN

[5]Cancer Biology Department, Vanderbilt University, Nashville, TN

[6]Vanderbilt-Ingram Cancer Center, Vanderbilt University, Nashville, TN

[7]Medical and Research Services, Department of Veterans Affairs, Tennessee Valley Healthcare System, Nashville, TN, USA

Germinal centers (GCs) promote humoral immunity and vaccine efficacy. In GCs, antigen (Ag)-activated B lymphocytes proliferate, are selected for high affinity antibody (Ab), promote Ab class switching, and yield B cell memory[1, 2]. Whereas the cytokine milieu has long been known to regulate effector functions that include the choice of immunoglobulin class [3, 4], both cell-autonomous[5] and extrinsic[6, 7] metabolic programming have emerged as modulators of T cell-mediated immunity[8]. We now show that GC light zones are hypoxic and low oxygen (pO_2) alters B cell physiology and function. In addition to reduced proliferation and increased B cell death, low pO_2 impaired Ab class switching to the pro-inflammatory IgG2c Ab isotype by limiting expression of the cytosine deaminase AID. Hypoxia induces HIF transcription factors by restricting activity of prolyl hydroxyl dioxygenases (PHD), enzymes that hydroxylate HIF-1α and HIF-2α to destabilize HIF through binding of Von Hippel-Landau protein (pVHL)[7]. B cell-specific pVHL depletion led to constitutive HIF stabilization, decreased Ag-specific GC B cells and undermined the generation of high-affinity IgG, switching to IgG2c, early memory B cells, and recall Ab

Correspondence and requests for materials should be addressed to M. R. B. (mark.boothby@vanderbilt.edu).
*These authors contributed comparably to this work.

Author Contributions S.H.C., A.L.R, K.S., E. V., V.H., J.W.T., and M.R.B. conceived of and designed these experiments; M.R.B. coordinated the research. S.H.C and M.R.B analyzed all data, and wrote the manuscript, which K.S., J.W.T., and E.V. edited. S.H.C. performed and analyzed the immunohistochemistry and flow cytometry for detection of GC hypoxia. S.H.C. and A.L.R. performed and analyzed the results of adoptive transfer and immunization experiments. K.S. with S. H. conceived, performed, and analyzed RNA-Seq. M.W., A.L.R. and SHC performed class-switching experiments and analyzed their data. S.H.C., A.L.R., and T.C.B performed and analyzed the metabolic assays. All other experiments and analyses were performed by S.H.C. and A.L.R.

Author Information The authors declare no competing financial interests.

responses. HIF induction can reprogram metabolic and growth factor gene expression. Sustained hypoxia or HIF induction via pVHL deficiency inhibited mTOR complex 1 (mTORC1) activity in B lymphoblasts, and mTORC1 haploinsufficient B cells had reduced clonal expansion, AID expression, and capacities to yield IgG2c and high-affinity Ab. Thus, the normal physiology of germinal centers involves regional variegation of hypoxia, and HIF-dependent oxygen sensing regulates vital functions of B cells. We propose that restriction of oxygen in lymphoid organs, which can be altered in pathophysiological states, modulates humoral immunity.

The micro-anatomy of secondary lymphoid organs and rapid proliferation of activated lymphocytes in them[9] prompted testing for hypoxia. Using flow cytometry, HIF levels were found to be increased in GC-phenotype B (GCB) cells compared to other B lymphocytes in spleens of immunized mice (Fig. 1a; Extended Fig. 1a). Immune fluorescent microscopy revealed that HIF was most elevated in germinal centers (Fig. 1b; Extended Fig. 1b). Low oxygen induces HIF. However, HIF α subunits can be stabilized at normoxic pO_2[10], so we used chemical probes to mark hypoxic cells in vivo. Spleen, lymph nodes, and Peyer's Patches were analyzed after injection of pimonidazole or EF5[11] and staining with Ab that bind the adducts (Fig.1c–e; Extended Data Fig. 1b–h). Fluorescence denoting hypoxia localized predominantly to the GC and the signal for each agent was weaker in the IgD^+ zone[1]. Flow cytometry detected EF5 only with $GL7^+$ GCB cells (Fig. 1e), and a hypoxia-related gene signature was enriched in GC B cells (Extended Data Fig. 1i). The EF5 and pimonidazole signals only partially filled GC, which are subdivided into light and dark zones between which B cells cycle iteratively to promote high-affinity Ab. EF5 labeling predominantly overlapped a follicular dendritic cell marker (CD35) restricted to the light zone (Fig. 1f). B lymphoblasts proliferate rapidly in the dark zone, whereas cell cycling decreases in the light zone[1]. The most EF5-positive GCB cells had entered S-phase at lower rates (% $BrdU^+$) (Fig. 1g, h) and more frequently activated an executioner caspase (Fig. 1i). Thus, activated B cells experience hypoxia in GC, predominantly in their light zones. Strikingly, the more hypoxic GCB cells proliferated less and had increased apoptotic signaling.

To test what impact hypoxia has on Ab class switching, activated B cells cultured in hypoxia (pO_2 of 1%) were compared to controls cultured at atmospheric (~21%) or venous (5%) pO_2, using conditions that promote IgG1 or the pro-inflammatory isotype IgG2c (Fig. 2a; Extended Data Fig. 2). Hypoxia restricted B cell population growth (Fig. 2a, b), with increased caspase-3 activation and lower BrdU incorporation (Extended Data Fig. 2a, b). Thus, O_2 sufficiency promoted B cell proliferation by both improving survival and increasing cell cycling. These effects were paralleled by an altered balance in cell metabolism, as hypoxia promoted a higher glycolytic rate (Extended Data Fig. 2c) in activated B cells. Conversely, PHD inhibition in vitro reduced O_2 consumption, and gene expression profiling of fresh ex vivo B cells showed major differences between non-GC and GC subsets (Extended Data Fig. 2d, e, respectively). Moreover, IgG^+ B cell frequencies were reduced at 1% pO_2 (Fig. 2a; Extended Data Fig. 2f). The enteric immune system is a site of physiological hypoxia[12]; notably, hypoxia did not decrease the frequency of IgA^+ B cells in IgA-promoting conditions (Fig. 2a; Extended Data Fig. 2f). Switching requires multiple B cell divisions[13]. When fluorescein partitioning was analyzed along with

switching to IgG2c, hypoxia reduced switching by B cells at the same division number (Fig. 2b). Thus, hypoxia at levels of the GC light zone altered Ab class switching by a direct influence on class choice in addition to reducing proliferation and reprogramming B cell metabolism and survival.

CSR is executed by an activation-induced deaminase (AID), encoded by the *Aicda* gene[1, 3, 4]. In IgG switch conditions, *Aicda* mRNA and AID protein were reduced by hypoxia (Fig. 2c, d; Extended Data Fig. 2g). In contrast, AID was not reduced by hypoxia in IgA switch conditions (Fig. 2d). Switch recombinase is directed to Ig heavy chain regions by transcription factors that create accessibility marked by germ line transcripts (GLT)[3, 4]. Hypoxia decreased induction of the transcription factor T-bet and the T-bet-dependent Iγ2c GLT[14] (Fig. 2e, f), whereas *Rora* mRNA and the GLT Iα were not reduced in B cells at reduced pO_2 (Fig. 2e, f). DMOG reduced proliferation and increased apoptosis of B cells cultured at 21% pO_2 and severely restricted switching to IgG2c, whereas that to IgA exhibited less impairment (Extended Data Fig. 3a, b). An inhibitor of HIF stabilization mitigated the reduction of IgG2c-switched B cells by low oxygen (1% pO_2) (Extended Data Fig. 3c). Akin to hypoxia, PHD inhibition and HIF stabilization impaired AID, T-bet, and Iγ2c GLT induction in the presence of the IgG2c switch cytokine IFN-γ (Fig. 2c, e, f; Extended Data Fig. 4a–c). In contrast, RNA for RORα and the Iα GLT were higher in DMOG-treated cells than in controls (Fig. 2c). Thus, hypoxia reduced AID and GLT induction in the conditions promoting IgG2c whereas Iα and AID levels were maintained in IgA conditions, consistent with relative effects on class-switched B cell antigen receptors (BCR).

pVHL destabilizes HIF by targeting hydroxylated alpha subunits for rapid proteasomal degradation in most oxygen-sufficient environments[7, 15]. To model persistent hypoxic signaling in vivo, we used conditional *Vhl* loss-of-function experiments. Mature B cells subjected to *Vhl* deletion yielded less Ag-binding GCB cells after immunization, less IgG2c Ab, and a substantial decrease in cells secreting Ag-specific IgG2c in primary (1^0) responses (Fig. 3a–c; Extended Data Fig. 5, 6). Cycling between light and dark zone in GC promotes higher affinity Ab[16] so it was striking that for IgM and IgG1 pVHL depletion only impaired generation of high-affinity anti-NP Ab (Fig. 3b). The defect in 1^0 responses substantially reduced IgG2c of all affinities (Fig. 3b; Extended Data Fig. 6a), whereas Ag-specific IgA was unaffected (Extended Data Fig. 6b). The effects of pVHL depletion on IgG2c and high-affinity IgG1 Ab responses were HIF-dependent (Fig. 3b). Defects of Ab responses were heightened in recall (2^0) immunity when compared to 1^0 responses (Extended Data Fig. 5c, d compared to Fig. 3a). pVHL loss reduced the population of Ag-binding memory-phenotype B (B_{mem}) cells, an effect mitigated by concomitant HIF depletion (Fig. 3c, Extended Data Fig. 6d). *Aicda* mRNA induction in activated B cells was impaired in cells with elevated HIF due to reduced *Vhl* (Fig. 3d; Extended Data Fig. 4c, d). *Tbx21* mRNA and T-bet protein levels also were lower in pVHL-depleted B cells (Fig. 3d; Extended Data Fig. 4c). To test the significance of decreased AID and T-bet, we forced expression of these proteins in activated B cells. T-bet did not increase the frequency of IgG2c–positive B cells during PHD inhibition, though it bypassed the need for IFN-γ with control B cells (Fig. 3e, Extended Data Fig. 4e). In contrast, forcing AID expression normalized switching in these assays (Fig. 3e; Extended Data Fig. 4e). We conclude that the PHD/HIF/VHL axis regulates

the qualities of Ab responses, with modulation of AID levels as a major mechanism for hypoxic influence on the Ig class preferences.

B cell activation, CSR, and development into Ab-secreting cells are effected by receptors that stimulate the mammalian target of rapamycin (mTOR). Hypoxia and HIF-1 have been shown either to inhibit or enhance mTORC1 activity in tumor or endothelial cells[17, 18]. In hypoxic and DMOG-treated B cells, BCR engagement elicited less phosphorylation of proteins downstream from mTORC1 (Fig. 4a; Extended Data Fig. 7a). Depletion of pVHL also reduced BCR-stimulated mTORC1 by a HIF-dependent mechanism (Fig. 4b). Thus, hypoxia restrained mTORC1 in normal B cells. In vitro experiments suggest that HIF-mediated limitation of increased amino acid transport contributes to this effect. B cell activation increased leucine uptake and expression of transporters used for nutrient uptake; HIF stabilization impaired this induction (Extended Data Fig. 7b–e). Moreover, adequate supplies of leucine were crucial, and partially sufficient, for BCR re-activation of mTORC1 in B lymphoblasts (Extended Data Fig. 7f). HIF depletion did not completely restore either the Ab response or amino acid uptake to normal in pVHL-deficient B cells. However, two additional mechanisms previously shown to suppress mTORC1 were evoked in hypoxic B cells in vitro – steady-state ATP pools were halved, accompanied by increased AMPK activity, and expression of the *Redd1* gene increased (Extended Data Fig. 8a–c).

Disruption of mTOR function by means that impair both mTORC2 and mTORC1 altered the balance between class-switched and IgM Ab against specific Ag[19, 20]. In contrast, HIF stabilization only partially inhibited mTORC1 and spared mTORC2 (Extended Data Fig. 8d, e). Accordingly, we tested if partially reduced mTORC1 activity impacts high-affinity Ab production, proliferation, AID levels, or biases of Ig class switching using disruption of *Rptor*, which encodes a protein essential for mTORC1[21]. *Rptor* haplo-insufficiency in B cells reduced mTORC1 activity (Extended Data Fig. 9a) and yielded results of in vitro switching and humoral responses in vivo (Fig. 4c, d; Extended Data Fig. 9) similar to those obtained with hypoxia and the PHD/HIF/VHL axis. IgG2c reductions were more substantial than those of IgM or IgG1 (Fig. 4c), and NP-specific GC B cells and IgG2c anti-NP Ab-secreting cells (ASC) (Extended Data Fig. 9b–d) were reduced. Partial mTORC1 loss reduced switching to IgG2c (Extended Data Fig. 10a) and suppressed high-affinity IgG1 Ab production (Fig. 4d). IgG1 switch conditions promoted higher expression of a tracking allele, AID-GFP, which was partially reduced by *Rptor* hemizygosity (Fig. 4e), whereas IgG2c conditions led to less AID in control cells and greater reduction in *Rptor* +/Δ B cells. Moreover, *Rptor* haploinsufficiency led to reduced T-bet, and decreased both *Tbx21* and *Aicda* mRNA in activated B cells (Extended Data Fig. 10b, c). Pharmacological inhibition of mTOR with rapamycin substantially reduced AID levels (Fig. 4f)[19, 20] and switching to IgG2c, an effect mitigated by forced AID and T-bet expression (Extended Data Fig. 10d–f). Overall, localized hypoxia and HIF induction are normal features of germinal center micro-physiology that modulate the output from lymphoid follicles, effects similar to those of restricting mTORC1 activity.

Low oxygen confronts B cells in germinal center during an immune response. The findings reveal that restricted oxygen supply or persistent induction of HIF transcription factors in B cells limits proliferation, isotype switching, and levels of high-affinity Ab. GC B cells

undergo iterative selection to enhance antibody affinity[1, 2] so that the most suitable B cells survive, further mature, and continue to multiply. Thus, the restriction of pO_2 of the GC may slow proliferation and set a more stringent threshold for critical survival signals. In addition, the IgG2c isotype has particular functions in anti-microbial responses and inflammation due to the affinities of its constant region with the spectrum of Fc receptors on cells[22]. Many patients suffering from hypoxemic lung disease exhibit lower serum IgG and heightened susceptibility to respiratory infection[23]. Hypoxia also has been recognized as a major aspect of inflammation in disease states. Intra-tumoral restrictions of oxygenation elicit indirect effects on immune function in cancer and may also act directly on T lymphocytes[24, 25]. Moreover, hypoxia and neo-lymphoid tissue or tertiary lymphoid structures with GC, plasma cells, and local Ab production are now recognized in a wide range of inflammatory settings whose oxygen landscape is unexplored[26]. The hypoxia response program in intestinal epithelial cells limits local inflammation[12, 27, 28], providing counter-regulation against activated neutrophils[27]. Analogous to this, the susceptibility of IgG2c to hypoxia may represent another means for limiting pathology from unchecked inflammation in normal immunity.

Methods

Mice and B cell transfer models

Mice [C57BL/6 mice, CD45.1 congenic, Ig C_H allotype disparate, *Rag*^{0}, AID-GFP Tg, pVHL cKO (*Vhl*$^{fl/fl}$; ER^{T2}-Cre)[29], pVHL; HIF1α; HIF2α triple cKO (*Vhl*$^{fl/fl}$;*Hif1a*$^{fl/fl}$;*Epas1*$^{fl/fl}$;ERT2-Cre), and Raptor cKO (*Rptor*$^{fl/fl}$;ER^{T2}-Cre)[30]] were housed in ventilated micro-isolators under Specified Pathogen-Free conditions in a Vanderbilt University mouse facility and used at 6–8 wk of age following approved protocols. Healthy mice of useful genotype were randomly selected for the experiments, without preference to size, gender, or other potential confounding factor. All Figures are based on data reproduced in independent biological replicates, typically conducted weeks or months apart in time and involving different cages of donor and recipient mice, and always with parallel handling and manipulation of the mice and cells of samples to be compared. For adoptive transfer experiments, B cells (from 1–2 donor mice of each genotype) were purified by depleting T cells using biotinylated anti-Thy1.2 Ab followed by streptavidin-conjugated microbeads (iMag™; BD Biosciences, San Jose CA). Pooled WT CD4$^+$ T cells and OT-II CD4$^+$ T cells (4 and 1 × 10^6 cells per recipient, respectively, typically from two donor mice of each background) were purified by positive selection with L3T4 anti-CD4 microbeads and, in adoptive transfers into *Rag*^{0} or Ig CH allotype-disparate (IgH^a) mice, mixed with pools of WT, *Vhl*$^{Δ/Δ}$, *Vhl*$^{Δ/Δ}$;*Hif1a*$^{Δ/Δ}$;*Epas1*$^{Δ/Δ}$, *or Rptor*$^{Δ/+}$ B cells (5 × 10^6 cells per recipient) and injected intravenously (i.v.) into *Rag*^{0} or IgH^a recipients. Recipient mice of similar ages (6–8 wk) were randomly selected for the experiments, without preference to size or gender. Experiments using the conditional *Vhl* alleles (*Vhl*$^{Δ/Δ}$) were designed to avoid distortions rapidly imposed by systemic pVHL loss [e.g., extra-medullary hematopoiesis[29]]. Those using *Rptor*$^{f/f+}$drove excision with the same *Rosa26*-CreERT2 allele and with tamoxifen-initiated Cre activity so as to be more directly comparable to the *Vhl* experiments and because of distortions of B cell development observed even for heterozygotes with *mb1*-Cre

(deletion at outset of B lymphoid ontogeny) (Raybuck, A.L. and M. Boothby, unpublished observations).

Reagents

IFN-γ, IL-4 and mAb (purified, biotinylated, or fluorophore-conjugated) were from BD Pharmingen or Tonbo Biosciences (San Diego CA) unless otherwise indicated. IL-5 was from Peprotech (Rocky Hill NJ), TGF-β and BAFF were from R&D Systems (Minneapolis, MN). NP-BSA (for capture ELISA), NP-OVA, and NP-O-succinimide were obtained from Biosearch (Novato CA). SRBC (sheep red blood cells), D-glucose, and 2-deoxyglucose were from Thermo Fisher Scientific (Waltham MA). Tamoxifen, 4-hydroxy-tamoxifen, chicken ovalbumin, all-trans retinoic acid and LPS were from Sigma-Aldrich Chemicals (St. Louis MO). DMOG and oligomycin were from EMD Millipore (Billerica, MA). Fluorescent proteins APC and rPE (Prozyme, Haward CA) were used for conjugation reactions with NP-O-succinimide to generate fluor-conjugated NP.

Immunohistochemistry and detection of hypoxia

C57BL/6 mice were immunized with SRBCs (2×10^8 cells per mouse). At 1 week after immunization, mice were injected with EF5[31] or pimonidazole HCl (Hypoxyprobe™) (Hypoxyprobe, Burlington, MA). Spleen, LN, and Peyer's Patches were embedded in OCT reagent and snap frozen on dry ice. Sections of frozen tissue were fixed with 4% paraformaldehyde, permeabilized with 0.5% Triton X-100 in PBS, blocked with M.O.M™ (Vector Lab) followed by incubation with GL7-FITC, IgD-PE, and anti-EF5-Cy5 Abs at 4 °C. For Hypoxyprobe™ detection, frozen sections were stained with biotinylated anti-pimonidazole Ab followed by streptavidin-conjugated Alex647 Ab. Biotinylated anti-CD35 Ab (BD Pharmingen, clone 8C12) followed by streptavidin-conjugated PE Ab was used for indirect immunofluorescent detection of FDC. Quantification of HIF-1α, EF5 and Hypoxyprobe™ fluorescent intensity within GC (total or light zone as defined by CD35 staining) and follicular regions was performed using MetaMorph Image processing software. For both negative controls and samples, the regions were quantified in toto using the signal-averaged fluorescence intensity within each boundary (e.g., $CD35^+$ or $GL7^+$) After subtracting the background MFI from negative control samples, MFIs of HIF-1α, EF5 and Hypoxyprobe™ within GC ($CD35^+$ and $CD35^{neg}$ zones) and GL7-negative follicular region were obtained. Data are presented as average (± SEM) MFI for the individual samples (n>20 GC for each condition, drawing evenly on three independent experiments). In flow cytometric detection of hypoxic cells, BrdU incorporation, or cleaved caspase 3, cell surface markers were stained by fluor-conjugated mAb, followed by fixation (4% paraformaldehyde), permeabilization with saponin (0.2%), and stained with anti-EF5-Cy5, or 2-step staining of pimonidazole according to supplier's instructions. BrdU and cleaved caspase 3 were detected as described[32].

Immunizations, and measurements of Ab responses

After collection of pre-immune sera, mice were immunized with NP_{16}-ovalbumin (OVA) (100 μg intraperitoneally) in alum (Imject, Thermo Fisher Scientific, Waltham MA) as described[33]. Alternatively, this primary immunogen was mixed with NP-modified SRBC, followed by a boost with NP-ovalbumin in alum. Relative levels of anti-NP Ab in immune

sera were assayed by ELISA on serial dilutions binding to either NP20-BSA (high valency, to capture all affinities of Ab) or NP2 (low valency, to restrict binding to the high-affinity Ab). Specific classes or isotypes were then detected using the series of isotype-specific second Ab of the SBA Clonotyping System (Southern Biotech, Birmingham AL), as described[33]. Data for Ag-specific Ab are shown after subtraction of low OD values from pre-immune controls analyzed together with the immune sera and were separately determined to match values yielded by titration. Ab-secreting cells (ASC) were analyzed by ELISpot as previously described[33] and quantitated using an ImmunoSpot Analyzer (Cellular Technology, Shaker Heights OH). Ag-specific B cells were detected and enumerated using flow cytometry to score B lineage-marked cells binding to fluor (APC or rPE)-conjugated NP, using a dump channel (7-AAD and APC-conjugated mAb against IgD, F4/80, Gr1, CD11b, CD11c, CD4, and CD8) to exclude non-specific signal.

Gene expression profiling

Mice were injected with SRBCs and sacrificed 10 days post-immunization. Single cell suspensions from spleens were stained with α-B220 (RA3–6B2) and GL7. $B220^{+}GL7^{-}$ and $B220^{+}GL7^{+}$ splenocytes were sorted into Trizol reagent (Ambion). Total RNA was isolated from biological replicates and provided to the Vanderbilt VANTAGE shared resource for library construction and sequencing. Briefly, libraries were constructed from poly-adenylated RNAs and sequenced with an Illumina HiSeq 2500 on an SR-50 run aiming for 30M reads/sample. Reads were aligned to the mm10 mouse transcriptome using TopHat and differential gene expression was determined using Cuffdiff as previously described[34]. Gene set enrichment analysis (GSEA) was performed using software available from the Broad Institute (http://www.broadinstitute.org/gsea), which tested for enrichment based on hypergeometric distribution with respect to published gene signatures. For hypoxia regulated gene signature, GSEA plots comparing a gene set pre-ranked by $\log_2$ fold change in gene expression ($GL7^{+}$ $B220^{+}$ vs $GL7^{-}$ $B220^{+}$) to a hypoxia signature published by Eustace *et al*[35]. A significant enrichment was defined as having an FDR q value ≤0.05. The results of RNA-Seq have been deposited in the NCBI Gene Expression Omnibus database under accession code GSE77113.

In vitro B cell cultures for class-switched Ab production

Splenic B cells were purified (90–95%) by depleting T cells using biotinylated anti-Thy1.2 mAb followed by streptavidin-conjugated microbeads. For IgG1, B cells (0.5×10^{6} cells/ml) were activated with LPS or $F(ab')_2$ anti-IgM (Southern Biotechnology) and anti-CD40 (BD Pharmingen), cultured with BAFF and IL-4. For IgG2c, B cells (0.5×10^{6} cells/ml) were activated with LPS or anti-IgM and anti-CD40, cultured with BAFF and IFN-γ. For IgA, B cells (0.5×10^{6} cells/ml) were activated with LPS (1 μg/ml) or anti-IgM and anti-CD40 and cultured with BAFF (10 ng/ml), TGF-β (5 ng/ml), IL-4 (10 ng/ml), IL-5 (10 ng/ml), and all-trans retinoic acid (RA) (10 nM) in IMDM medium supplemented with 10% FBS, Pen/Strep, L-glutamine, and β-mercaptoethanol. To analyze the partitioning of cell division, purified B cells were stained with CellTrace™ Violet (Thermo Fisher Scientific) according to manufacturer's instruction or CFDA-SE as described previously[33]. Cells were cultured (4 d) at pO_2 of 21%, 5% or 1% after which surface Ig was analyzed by flow cytometry. In comparisons of all three [O_2] (oxygen tensions), experiments were performed by dividing

one common pool of B cells and using two separate hypoxia chambers maintained at constant pO_2 using nitrogen.

Measurements of RNA and proteins

RNA was isolated using Trizol reagent (Invitrogen). After cDNA synthesis by reverse transcription, expression of genes was analyzed in duplicate samples using SYBR green PCR master-mix (Qiagen, Valencia CA) by quantitative real-time RT-PCR (qRT^2-PCR). Data are presented as values normalized to WT control and averaged over PCR normalized to levels of internal control (actin). Primer pairs are detailed in a Table that, along with conditions, is freely available upon request. Proteins in whole cell extracts were separated by SDS-PAGE, transferred onto nylon membranes (Millipore), and then incubated with rabbit antibodies against p-S6 (S235/236), p-p70S6K (S371), p-Akt (S473), p-Akt (T308), p-ACC (S79), p-AMPK (T172) (Cell Signaling Technologies), or goat anti-Actin (Santa Cruz) Abs followed by the appropriate fluorophore-conjugated, species-specific secondary anti-Ig antibodies (Rockland Immunochemicals, and LI-COR). Proteins were visualized and quantitated by laser excitation and infrared imaging (Odyssey, LI-COR). For measurements of the induction of S6K, S6 and Akt phosphorylation, purified B cells were cultured 2 d in BAFF (10 ng/ml) and $F(ab')_2$ anti-IgM (1 μg/ml), washed, rested 18 h, and then re-stimulated (15 min) in the presence or absence of $F(ab')_2$ anti-IgM (2.5 μg/ml). To test the effect of amino acid supply on S6K and S6 phosphorylation, B lymphoblasts were washed, cultured in complete medium overnight, then rinsed, cultured in amino acid-free RPMI1640 (US Biological, Salem, MA) for 1 hr, and re-stimulated in the presence or absence of anti-IgM, with readdition of L-leucine (Sigma) or all 20 amino acids. For the induction of p-ACC and p-AMPK, purified B cells were cultured for 2 d in LPS, BAFF, and IFN-γ.

Glycolysis and oxygen consumption assays

Purified B cells were cultured for 2 d at 37°C at pO_2 of 21% (normoxia) or pO_2 of 1% (hypoxia) in the presence of BAFF, LPS, and IFN-γ. To quantitate glycolysis, 1×10^6 viable cells were washed, pulsed with 10 μCi of 5-[^{3}H]-glucose in 24-well plates (37°C, 1 h), and returned to their previous oxygen condition. Glycolytic conversion was then quantitated as described[32]. Oxygen consumption rates were measured using Seahorse assays. Because this instrument cannot be used in a hypoxia chamber, purified B cells (1×10^6 cell/ml) were activated with 1 μg/ml LPS and cultured 48 hr with 10 ng/ml BAFF in complete IMDM medium supplemented as described[32] in the presence or absence of 0.5 mM DMOG. After 48 hr, cultured B cells were washed twice, resuspended in XF Base Media (Seahorse Bioscience, North Billerica MA) supplemented with 2 mM L-glutamine, and equal numbers of Trypan Blue-excluding B cells (1.5×10^5) were plated on extracellular flux assay plates (Seahorse Bioscience) coated with CellTak (Corning) according to the manufacturer's protocol. Before extracellular flux analysis, B cell were rested (25 minutes at 37°C, atmospheric CO_2) in XF Base Media. Oxygen Consumption Rate (OCR) and Extracellular Acidification Rate (ECAR) were measured using a XF96 extracellular flux analyzer (Seahorse Bioscience) before and after the sequential addition of 10 mM D-glucose, 1 μM oligomycin, and 50 mM 2-deoxyglucose.

Amino acid uptake assay

Purified B cells were activated and cultured 2 d with LPS and BAFF. Viable cells were washed and incubated with amino acid uptake buffer (5.4 mM KCl, 140 mM NaCl, 1.8 mM $CaCl_2$, 0.8 mM $MgSO_4$, 5 mM D-glucose, 25 mM HEPES, and 25 mM Tris, pH 7.5) for 30 min to deplete intracellular amino acids. Triplicate samples (1×10^6 cells/sample) were incubated with 1 μCi of L-[3, 4, 5-^{3}H] leucine (American Radiolabeled Chemicals, Inc) in amino acid uptake buffer for 2 min at room temperature and immediately spun through a layer of bromododecane (200 μl) into 8% sucrose/ 20% perchloric acid (25 μl). Tubes were frozen in a dry ice/EtOH bath and cut with dog nail clippers to separate the cells from unincorporated [^{3}H]-leucine. 25 ul of 10% Triton X-100 and liquid scintillation cocktail were added and the cell-associated ^{3}H were measured by liquid scintillation counting.

Statistical analysis

The primary analyses were conducted on pooled data points from independent samples and replicate experiments (minimum two, generally three, biologically and temporally independent replicate experiments for all data, with multiple independent samples in the case of two biological replicates), using an unpaired two-tailed Student's *t* test with post-test validation of its suitability. Welch's or Mann-Whitney testing were used instead of the t-test where indicated based on statistical analysis of the distribution of variances in the samples to be compared. Data are displayed as mean (± SEM), i.e., 'center values' were mean as 'average'. Results were considered statistically significant when the p value of for the null hypothesis of a comparison was <0.05. Since the extent or direction of difference between samples was unknown, and regulations mandate reducing the number of animals used to the lowest feasible level, no statistical methods were used to determine pre-specified sample sizes. The experiments were not randomized and the investigators were not blinded during the experiments. Corrections for multiple comparisons were not used. Statistical approaches for RNA-Seq-related data are outlined in that section.

Extended Data

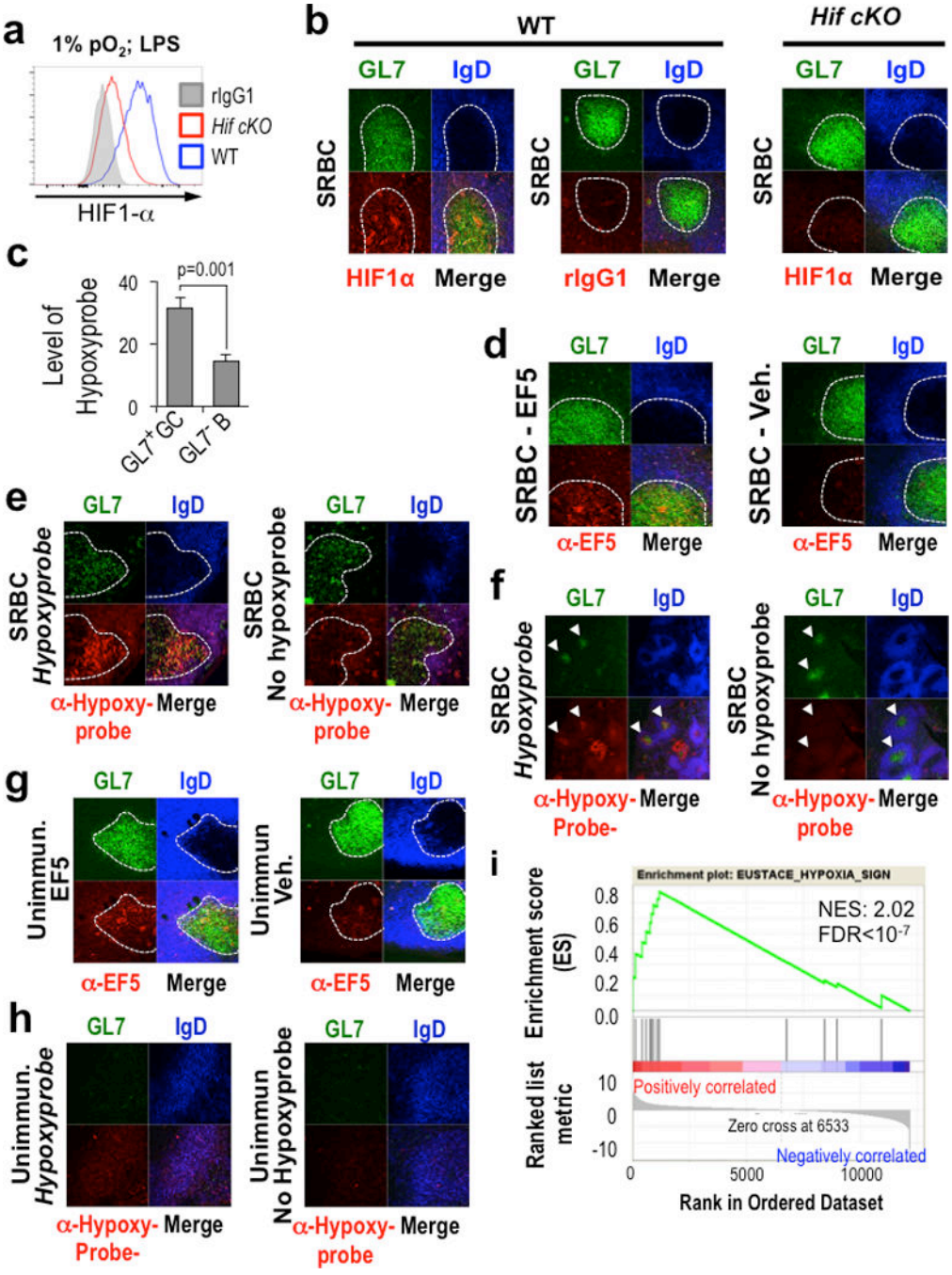

Extended Data Figure 1. Landscape of hypoxic cells in follicles and GCs of lymphoid organs

(a, b) Controls for anti-HIF-1α Ab staining of GC and portions of the surrounding splenic follicle, as in Fig. 1a, b, with fluorescent signals at the same intensity settings when analyzing samples processed together, using SRBC immunization of WT and *Hif*-deleted mice and either anti-HIF-1α sera or non-immune rabbit IgG (rIgG1), as indicated. Shown are (a) flow cytometry results of intracellular staining performed after exposure of lymphoblasts of the indicated genotypes to 4-hydroxytamoxifen and hypoxia, and (b)

confocal images (40x magnification) as in Fig. 1a, b, respectively. (c) Quantified data obtained from samples represented in Fig. 1c. Shown are the mean (±SEM) specific fluorescence intensities of Hypoxyprobe™ (anti-pimonidazole) staining in germinal centers (delimited as $GL7^+$) and $GL7^-$ IgD^+ follicular B cell regions after subtracting background signal (mean fluorescence intensities in these regions after anti-pimonidazole staining of samples from PBS-injected control mice). (d) Immunostaining of EF5-modified cells. Shown are confocal microscopic images of spleen sections from SRBC-immunized mice injected with EF5 (left) or PBS (right) 2 hr before harvest, followed by direct immunofluorescent staining of frozen sections with anti-GL7 Ab, anti-IgD and anti-EF5, representative of the quantified data presented in Fig. 1d. (e) Representative images of mesenteric LN after injections and immunostaining as in Fig. 1c. (f) Low (10x) magnification image of anti-pimonidazole immunohistochemistry on spleen sections from SRBC-immunized mice injected with pimonidazole (left) or PBS (right) prior to harvest. Among stained sections for both anti-pimonidazole and EF5, ~75 % of GC sections were unequivocally positive. (g) Representative images of Peyer's Patches from non-immune, EF5-injected mice processed as in Fig. 1c. (h) Representative images of spleen sections from unimmunized mice injected with Hypoxyprobe™ (left) or PBS (right) 3 hr before harvest, processed in parallel with sections from immunized mice injected with probe, and imaged by confocal microscopy at the same time and settings as for the sections from immunized mice. (i) GSEA plots comparing gene set pre-ranked by $\log_2$-fold change in relative expression ($GL7^+$/GL7-) in a hypoxia gene signature.

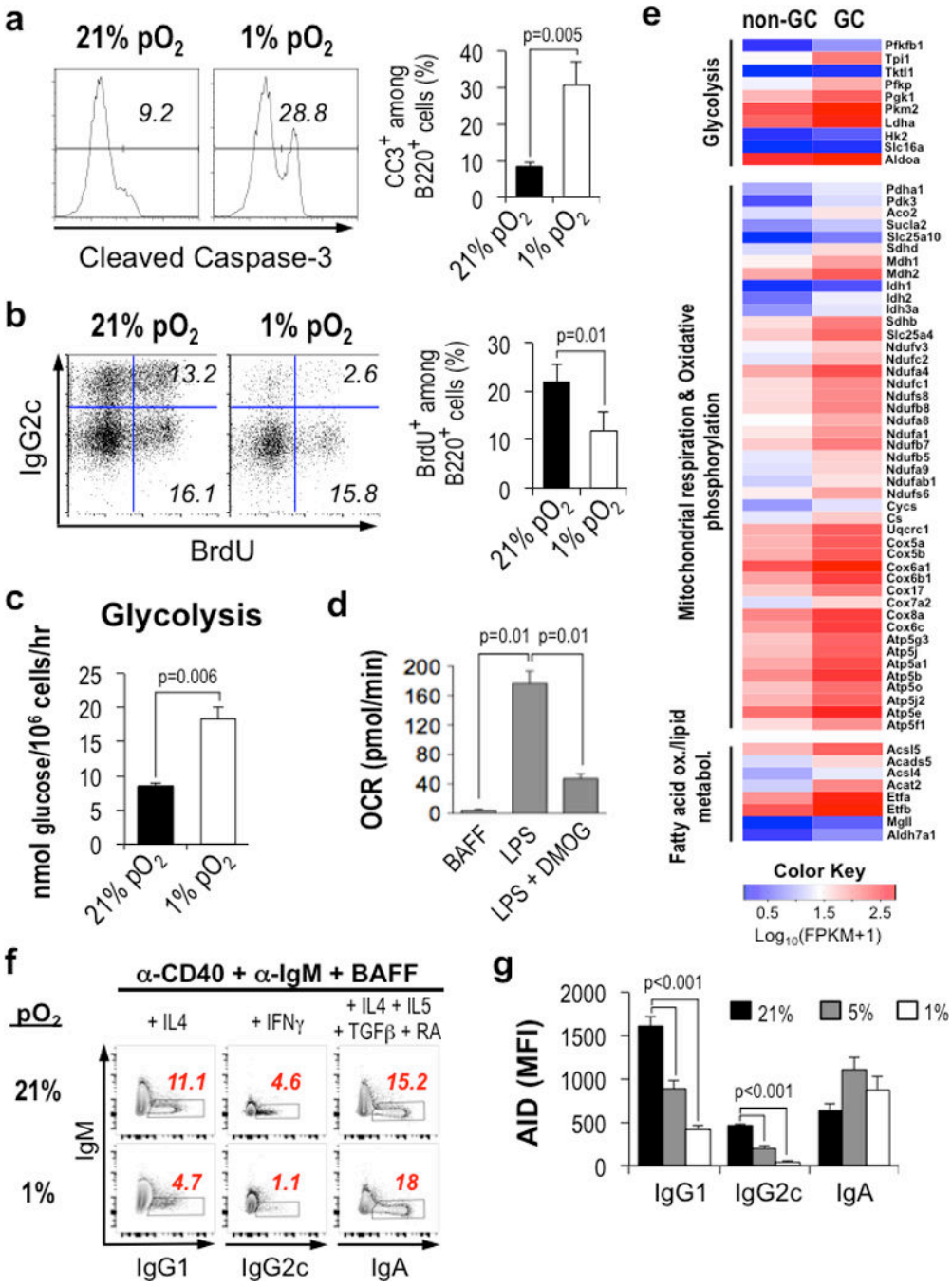

Extended Data Figure 2. Altered B cell survival, proliferation and metabolism in reduced pO_2

(a) Increased executioner caspase-3 activation in hypoxic B cells. Shown (left panels) are representative flow histograms of activated (cleaved) caspase-3 (CC3) in the B cell gate after activated B cells were cultured in pO_2 of 21% (normoxia) and 1% (hypoxia). B cells were stimulated with BAFF, LPS, and IFN-γ, cultured (4 d) at the indicated oxygen tension and processed for detection of activated caspase-3 using fluorescent-conjugated active caspase-3 Ab. Panel to right displays the mean (±SEM) quantitative data for the frequencies of B cells positive for caspase-3 cleavage in three independent replicate experiments. (b) O_2

sufficiency enhances cell cycle rates. As in (a), but cells were pulsed with BrdU and frequencies of S-phase during the cultures are displayed in relation to IgG2c switching, with a representative result (left panels) and quantitation of the overall $B220^+$ cell populations in three independent replicate experiments (right panel). B cells were cultured (4 d) with BAFF, LPS, and IFN-γ at the indicated oxygen levels, pulsed (4 hr) with BrdU, and then stained with anti-IgG2c, -B220, and -BrdU Ab after fixation, permeabilization, and processing. (c, d) Pools of purified WT B cells were stimulated with BAFF and LPS, divided, and cultured (2 d) in pO_2 of 21% (normoxia) and 1% (hypoxia). (c) Rates of glycolysis were measured after return to their previous oxygen conditions, using equal numbers of surviving B cells after culture as detailed in the *Methods*. The bar graph shows mean (±SEM) rates of glycolysis measured in three independent experiments. (d) Inhibition of PHD activity decreases cellular respiration of B lymphoblasts. Purified B cells were activated and cultured (2 d) with LPS and BAFF in the presence or absence of the PHD inhibitor DMOG (0.5 mM). Oxygen Consumption Rate (OCR) was measured with cultured viable B cells (1.5×10^5 cells) as detail in the *Methods*. The bar graph shows mean (±SD) OCR of technical triplicate measurements in one experiment representative of three independent replicates with similar results. (e) Metabolic gene expression profile of $GL7^+$ GC B cells. Genes showing significant expression changes in $GL7^+$ GC B cells were mined for genes important for the indicated cellular processes. The heat map depicts values for the indicated genes shown as the value derived as $\log_{10}$ of the fragments per kilobase per million (reads) after adding 1 to each value (FPKM+1). (f) Hypoxia limits switch to IgG among B cells activated via BCR and CD40. As in Fig. 2a, except that the B cell preparations were activated by cross-linking their surface IgM and CD40 without addition of LPS. (g) Quantified mean fluorescence intensities for GFP expression in the full set of replicate experiments conducted as in Fig. 2d, presented as mean (±SEM) data for each condition of culture (pO_2 of 21, 5, or 1%, with cytokines and retinoic acid for Ig class switch conditions as indicated, and as for Fig. 2a, b).

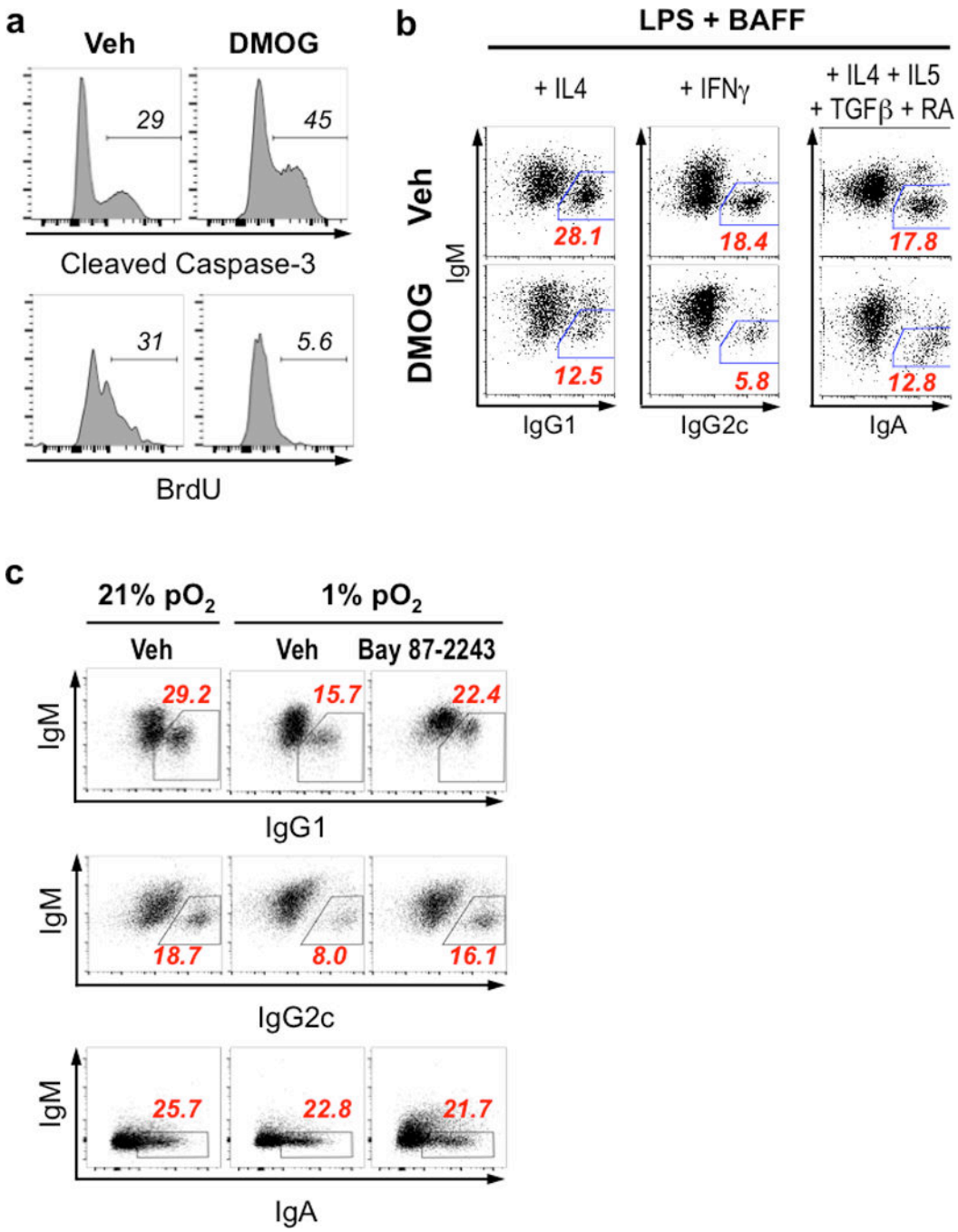

Extended Data Figure 3. HIF stabilization alters B cell survival, proliferation and class switched Ab level

(a) Purified WT B cells were activated and cultured (4 d) with LPS and BAFF in the presence or absence of DMOG, after which frequencies of cells with cleaved caspase 3 or BrdU uptake, as indicated, were measured as in Extended Data Fig. 2 (representative result from one experiment among n=3 independent replicate experiments). (b) Purified WT B cells were activated and cultured in conditions for switching to IgG1, IgG2c, and IgA, as in Fig. 2a, b, but at atmospheric (21%) pO_2 in the presence or absence of DMOG, after which the frequencies of surface IgG1, IgG2c and IgA among $B220^+$-gated cells were measured as

in Fig. 2 and detailed in the Methods. FACS plots display the surface levels of IgG1, IgG2c, and IgA on $B220^+$-gated cells in one experiment representative of three independent replicates. (c) HIF inhibition impedes the hypoxia-induced alteration of Ab class switch choices. B cells were activated and cultured (4 d) with BAFF, LPS, and the indicated switching condtions as in Fig. 2a (IL-4, IgG1; IFN-γ, IgG2c; retinoic acid, TGF-β, IL-4 and −5, IgA) at pO_2 of 21% (normoxia) or 1% (hypoxia) in the presence or absence of the HIF inhibitor Bay 87–2243. FACS plots displaying the surface levels of IgG1, IgG2c, and IgA on $B220^+$-gated cells in one representative result among three independent experiments are shown.

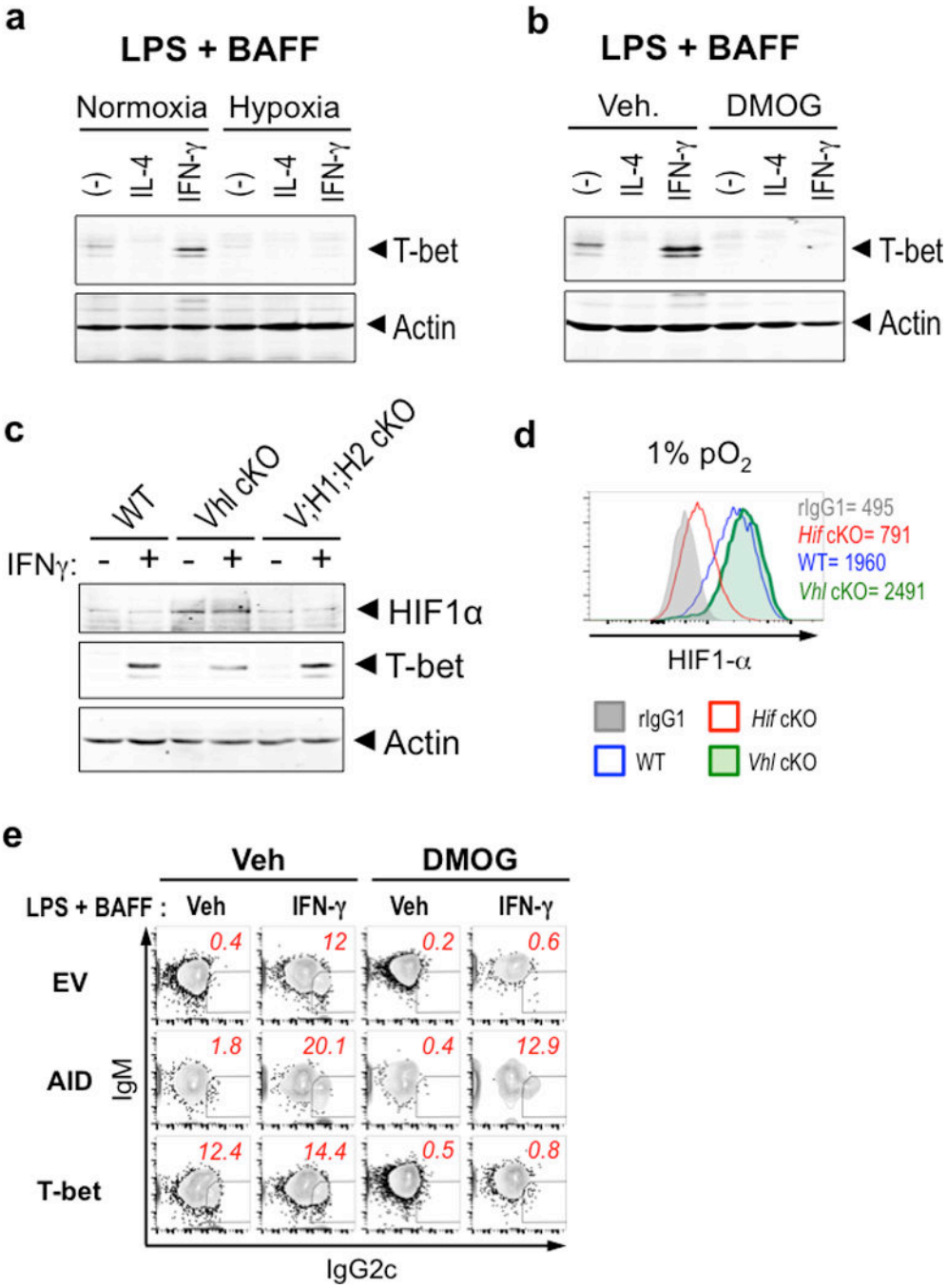

Extended Data Figure 4. Hypoxia and PHD inhibition repress T-bet induction

(a, b) B cells from WT mice were activated and cultured in LPS, BAFF, and IL-4 or IFNγ for 4 days under normoxic and hypoxic conditions (a) or cultured with and without DMOG at pO_2 of 21% (b). Shown are results of immunoblots using anti-T-bet Ab along with actin as a loading control. Data are one representative result from among three independent experiments. (c) HIF-dependent regulation of T-bet expression by pVHL. B cells from WT or conditionally deleted *Vhl* and *Vhl*; *Hif1a; Epas1* (*Vhl*, and V;H1;H2, respectively) cKO mice were activated and cultured (4 d) in LPS and BAFF in the presence or absence of IFN-

γ, as indicated. Results of one representative immunoblot (from among three independent experiments) probed for HIF1α, T-bet and actin are shown. (d) HIF superinduction by pVHL depletion in B cells at 1% pO_2. WT and B cells after conditional *Vhl* f/f deletion were activated, cultured in 1% pO_2 as in Extended Data Fig. 1a, and analyzed by flow cytometry after processing together for indirect immunofluorescent staining of intracellular HIF-1α as in Fig. 1a and Extended Data Fig. 1a. Numbers denote the mean fluorescent intensity of the B cells of each type. (e) Flow cytometric data from one representative experiment as in Fig. 3e, in which B cells were transduced with MIT, MIG, MIT-T-bet or pMx-GFP-AID retrovectors, and cultured with BAFF and LPS ± IFN-γ in the presence or absence of DMOG. The frequencies of surface $IgG2c^+$ events among $B220^+$ cells analyzed 4 d after transduction are shown, with flow data from one experiment of three independent experiments.

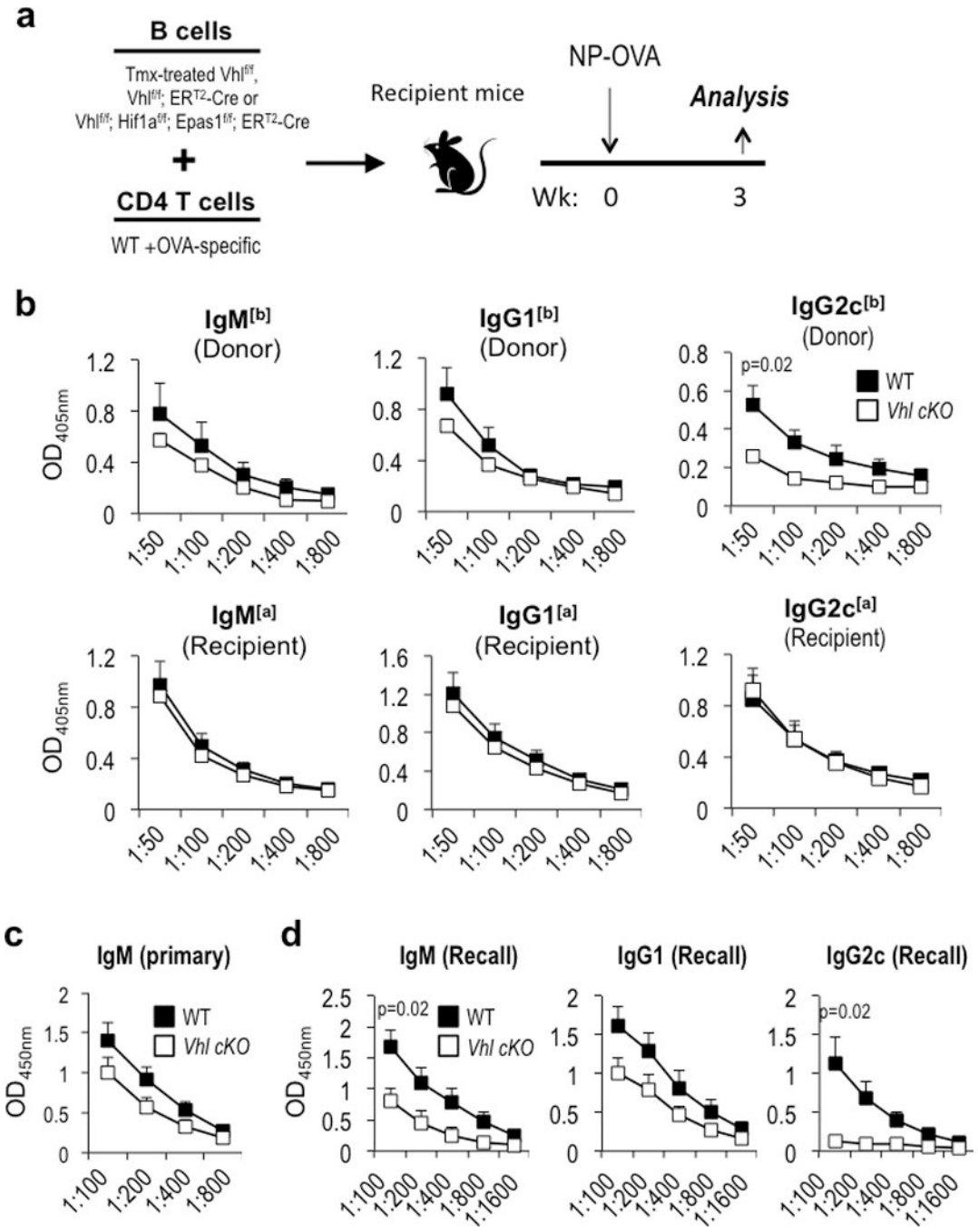

Extended Data Figure 5. VHL regulates Ag-specific Ab production

(a) Schematic outline of adoptive transfer experiments. B cells purified from tamoxifen-treated WT, *Vhl*$^{f/f}$, or *Vhl* $^{f/f}$; *Hif1a* $^{f/f}$; *Epas1* $^{f/f}$ CreER^{T2+} mice were transferred into recipients after mixing with CD4^{+} T cells (polyclonal : Ag-specific = 4:1). Recipients were analyzed after primary (1^0) immunization or, for memory responses, after the 1^0 and a recall immunization. (b) As in Fig. 3a, except B cells from WT or conditionally deleted *Vhl* cKO mice were mixed with CD4^{+} OT-II TCR transgenic T cells, transferred into Ig C_H allotype-disparate recipient mice, followed by immunization with NP-ovalbumin and harvest 3 wk

after primary immunization. Donor- ([b] allotype) and recipient-derived ([a] allotype) NP-specific IgM and IgG1 levels in the sera were analyzed by ELISA. The mean (±SEM) absorbance data averaging independent samples [n=8 (WT) and 7 (*Vhl* cKO)] obtained in two separate transfer experiments (measured on the same ELISA plate) are shown. (c, d) As in Fig. 3a, WT or *Vhl* Δ/Δ (*Vhl* cKO) B cells were mixed with WT $CD4^+$ T lymphocytes (a 4:1 mixture of polyclonal and OVA-specific OT-II cells), and transferred into *Rag*^{0} recipients that were then immunized with NP-ovalbumin, and analyzed for NP-specific Ab levels 3 wk after primary (1^0) immunization (c) or, for memory response, 9 wk after the 1^0 and 1 wk after a recall immunization (panel d). [n= 5 independent recipients per genotype in two independent experiments.] (c) Mean (±SEM) ELISA data for all-affinity IgM anti-NP from the same samples as Fig. 3b are shown. (d) Impaired immune memory follows interference with B cells' hypoxia response system. Terminal sera obtained from the recipient mice (Fig. 3a) 1 wk after recall immunization were analyzed by ELISA for all-affinity anti-NP Ab of the indicated isotypes at the same time as the 1^0 response samples (Fig. 3a; Extended Data Fig. 5c).

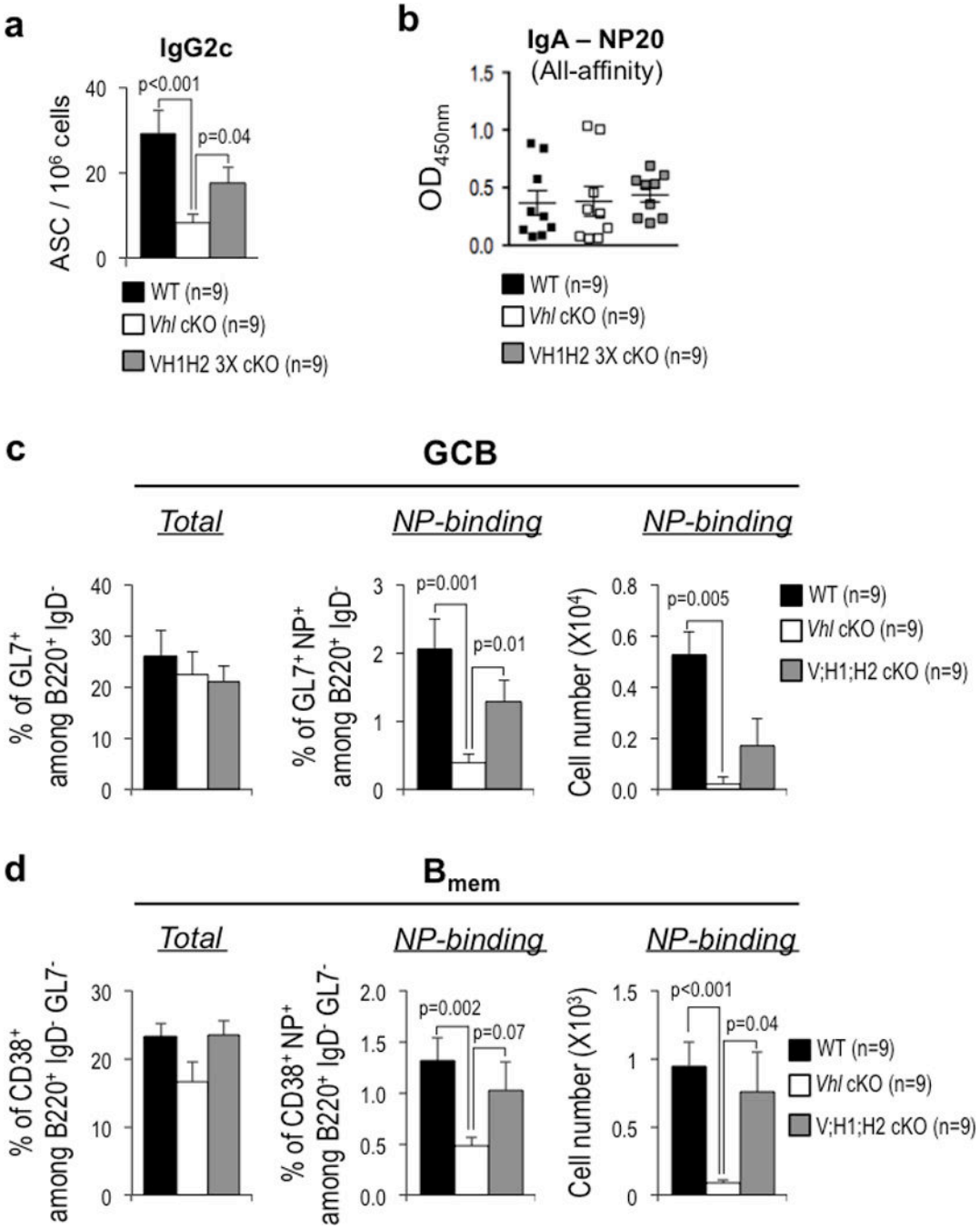

Extended Data Figure 6. HIF-dependent regulation of antigen-specific B cell population and antibody response by pVHL

(a, b) As in Fig. 3, WT, *Vhl* Δ/Δ ("*Vhl* cKO"), or *Vhl* Δ/Δ *Hif1a* Δ/Δ *Epas1* Δ/Δ ("V;H1;H2 cKO") B cells were mixed with WT $CD4^+$ T lymphocytes (a 4:1 mixture of polyclonal and OVA-specific OT-II cells), transferred into Rag^0 recipients that were then immunized with NP-ovalbumin and analyzed for NP-specific Ab levels after primary (1^0) immunization as in Fig. 3b, c. Using the same mice and samples as for Fig. 3b, c, cells in spleen secreting IgG2c anti-NP were quantified by ELISpot and averaged as frequencies of Ab-secreting cells (ASC) in the sample (a). Mean (±SEM) frequencies for all samples (n=9 each) are shown.

(b) Anti-NP IgA levels in the sera of the samples used in Fig. 3b were quantified by ELISA. (c, d) VHL regulation of Ag-specific GC and memory B cells is HIF-dependent. As in Fig. 3b, c, WT, pVHL-depleted (*Vhl* Δ/Δ , *Vhl* cKO), or pVHL, HIF-1α, HIF-2α-depleted (*Vhl* Δ/Δ *Hif1a* Δ/Δ *Epas1* Δ/Δ, "V;H1;H2 cKO") B cells were mixed with $CD4^+$ T cells (4: 1 polyclonal: OVA-specific), transferred into *Rag*^{0} mice, immunized with NP-SRBC along with NP-OVA, boosted with NP-OVA at 3 wk after primary immunization, and analyzed at 1 wk after the boost. Shown are the mean (±SEM) frequencies or numbers of Ag (NP)-binding B cells of GC- (IgD^- $GL7^+$) (c), and early memory (IgD^- $GL7^-$ $CD38^{hi}$) phenotypes (d) derived from each donor population and recovered in the recipient mice, as determined by enumeration and flow cytometric phenotyping with fluor-conjugated NP.

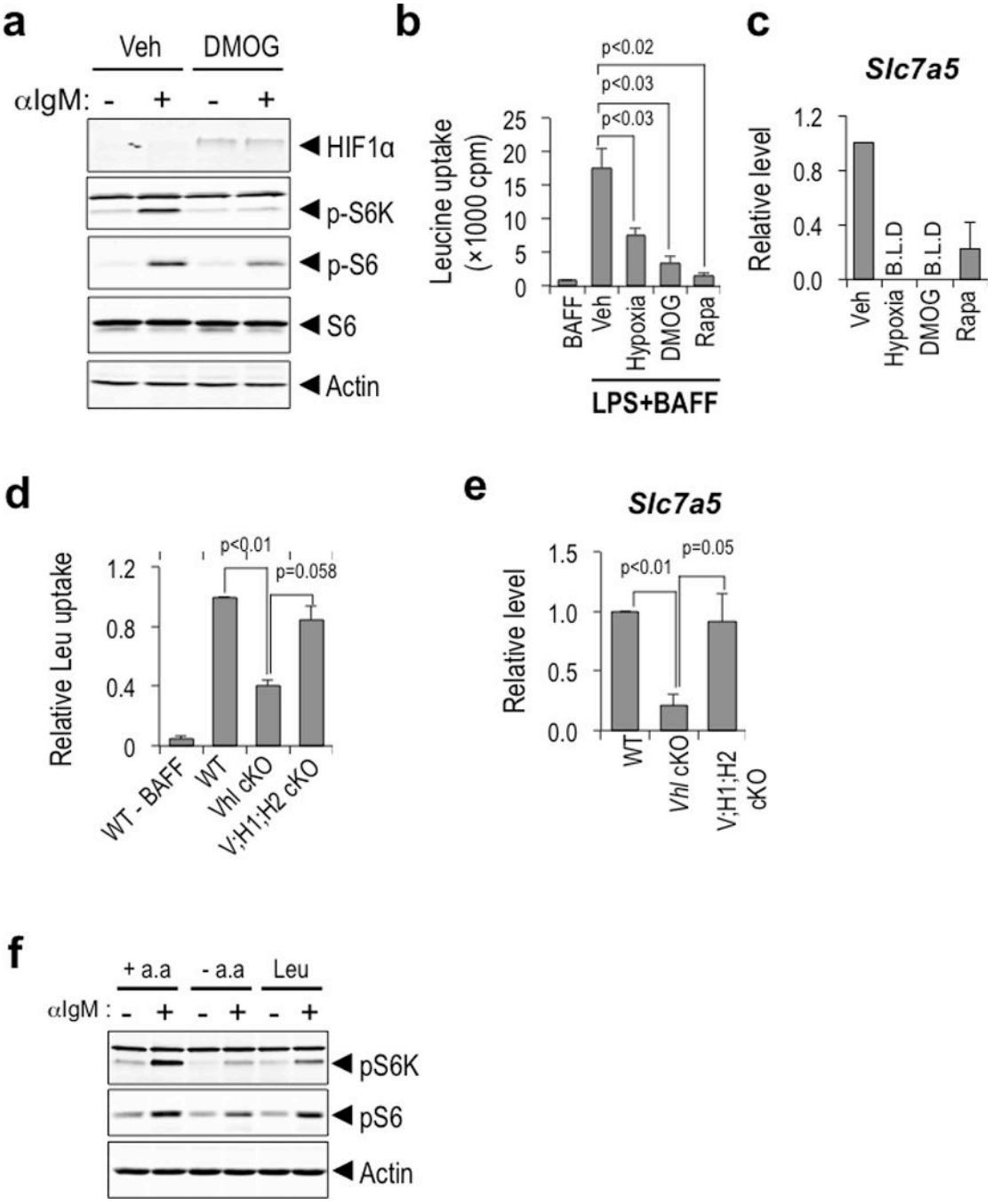

Extended Data Figure 7. Hypoxia interrupts impairs an activation-induced feed-forward loop in which mTORC1 increases leucine uptake by B cells

(a) PHD inhibition attenuates mTORC1 activity. WT B cells were activated with αIgM and cultured (2 d) in BAFF, rested 20 h in the presence or absence of DMOG, and then re-stimulated (20 min) with αIgM. Shown are immunoblots probed with anti-HIF1α, anti-p-S6K, anti-p-S6, and anti-S6 Ab along with anti-actin as a loading control. Data are the results from one representative experiment among three independent replicates. (b–f) Hypoxia and HIF stabilization reduce leucine uptake and mTORC1 activation. (b, c) Reduced leucine uptake (b) and *Slc7a5* mRNA encoding the large neutral a.a. transporter

LAT1 (c) with inhibition of PHD proteins or mTOR. WT cells were analyzed after culture in 1% O_2 or at pO_2 of 21%, in presence of vehicle, PHD inhibitor (DMOG), or mTORC1 inhibitor (Rapa) as indicated. (b) Mean (±SEM) B cell uptake of leucine, in n=3 independent experiments. (c) Mean (±SEM) relative mRNA level, normalized to actin (n=3 independent experiments). (d, e) Activated B cells of the indicated genotypes were assayed for leucine uptake (d) and induction of the *Slc7a5* gene encoding a large neutral a.a. transporter (e). (d) Mean (± SEM) leucine uptake by the cultured cells, normalized in each independent experiment (n=3) to activated WT cells. (e) VHL loss leads to HIF-dependent attenuation of *Slc7a5* mRNA levels. WT or cKO B cells of the indicated genotypes were activated and cultured at 21% O_2 as in Fig. 3d. Mean (± SEM) qPCR results normalized first to actin for level within a sample, and then to the WT control in each independent experiment (n=3). (f) Leucine stimulates mTORC1 activity in activated B cells. Activated WT B cells, divided and cultured overnight in medium lacking or sufficient for the indicated a.a., were restimulated and analyzed as in Fig. 4a, b.

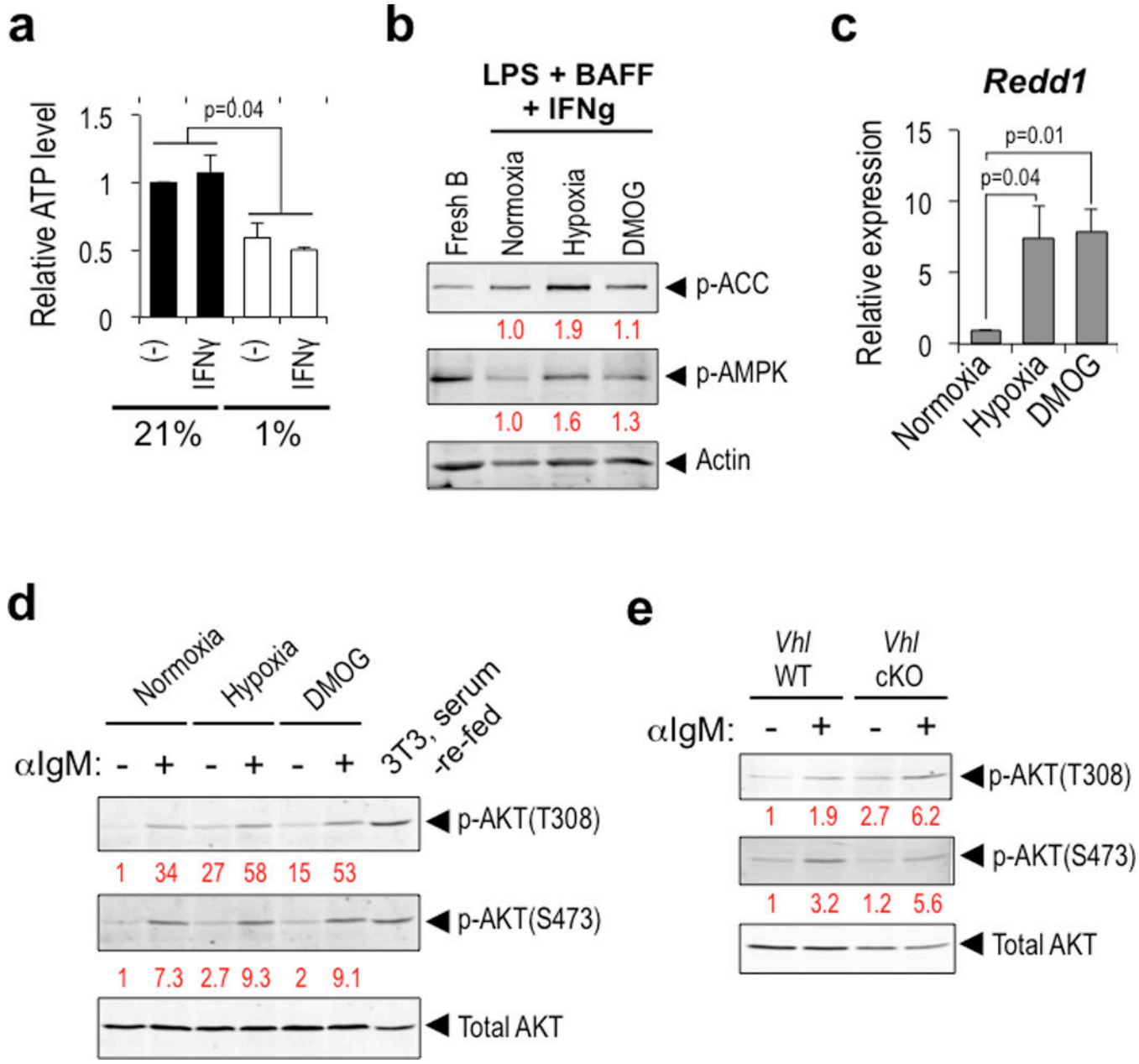

Extended Data Figure 8. Hypoxia promotes AMPK activity and induction of the mTORC1 inhibitor REDD1 without repressing mTORC2

(a) B cells were activated and grown (2 d) in LPS and BAFF at the indicated pO_2 and in the presence or absence of IFN-γ as indicated. ATP concentrations in equal numbers of cells were then assayed. In each of three replicate experiments with similar results, the [ATP] measured for cells at conventional (21%) pO_2 without IFN-γ was set as 1, and the mean (±SEM) levels in each sample relative to this reference are shown for three biological replicates. (b) Immunoblot results after probing membranes with anti-p-ACC, anti-p-AMPK(T172), and actin are shown for one representative experiment. Numbers indicate the level of signal for cells cultured in hypoxia or DMOG as compared to the reference value of the sample cultured in conventional (21%) pO_2, after normalization of each sample

according to its loading. (c) Results of a representative qRT^2-PCR experiment measuring *Redd1* mRNA in WT B cells (activated and cultured as in panel b), with each sample first normalized to *Actin* mRNA and then to vehicle-treated cells. (d, e) Effect of VHL, hypoxia, and DMOG on Akt phosphorylation in B cells. (d) B cells were activated with anti−IgM and BAFF, cultured (2 d) and rested (20 h) under conditions of hypoxia, or normoxia in the presence or absence of DMOG, after which cells were re-stimulated (20 min) with anti −IgM. (e) As in (d), B cells from WT or conditionally deleted *Vhl* cKO mice were activated with anti−IgM in the presence of BAFF, cultured (2 d) and rested (20 h), after which cells were re-stimulated (20 min) with anti−IgM. Shown are results of immunoblots probed with antibodies directed against p-Akt (T308), p-Akt (S473), and Akt. Numbers show the quantitation of signal relative to B cells that were not restimulated, after adjustment of each sample for loading as determined by total Akt. Data shown are from one representative experiment among three independent replicates.

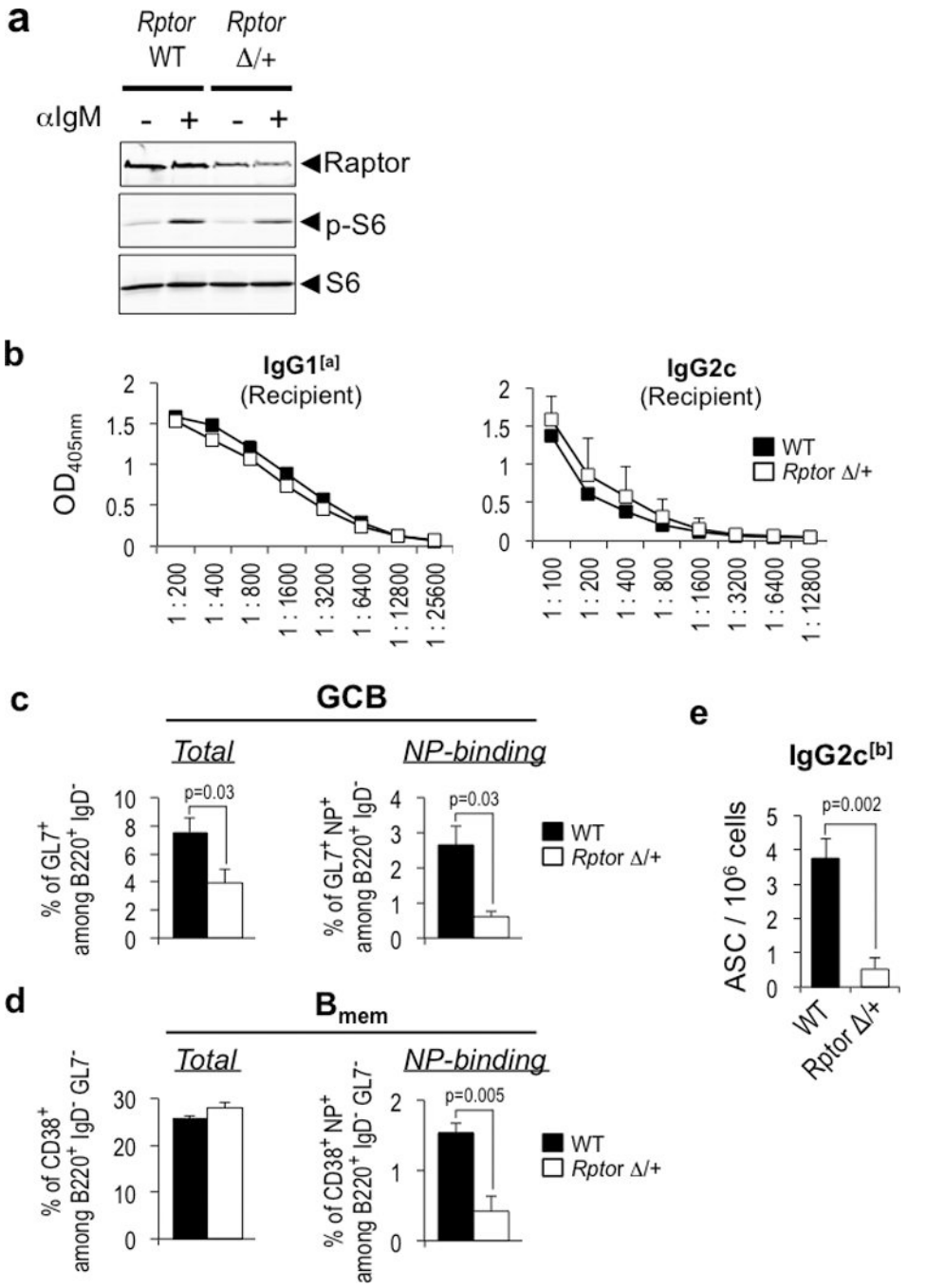

Extended Data Figure 9. mTORC1 regulates expansion of Ag-specific B cells and Ab class spectrum

(a) Results of immunoblots using anti-Raptor, and anti-p-S6 along with anti-S6 Ab as a loading control. B cells (WT or haploinsufficient for Raptor) were activated with $F(ab')_2$ anti −IgM and BAFF, cultured (2 d) and rested (20 h), after which cells were re-stimulated (20 min) with $F(ab')_2$ anti−IgM. Data are from one representative experiment among three independent replicates. (b) Recipient Ab controls for effect of mTORC1 on class-switched Ab responses. As in Fig. 4c, WT or Raptor-haploinsufficent B cells (from heterozygous mice that were ROSA26-CreERT2, *Rptor* f/+ and converted to Δ/+ by tamoxifen injections)

were mixed with $CD4^+$ OT^{II} TCR transgenic T cells, transferred into Ig C_H allotype-disparate recipient mice, immunized with NP-OVA, and harvested at 3 wk after primary immunization. Donor- ([b] allotype) (in Fig. 4) or recipient-derived ([a] allotype) NP-specific IgG1 and IgG2c levels in the sera were analyzed by ELISA. Mean (±SEM) absorbance data averaging samples [n=9 (WT) vs. 8 (*Rptor* +/Δ)] obtained in three separate experiments (measured on the same ELISA plate). (c–e) WT or *Rptor* Δ/+ B cells were mixed with $CD4^+$ T cells (polyclonal : OVA-specific = 4: 1) and transferred into Rag^{0} mice and immunized with NP-OVA. Shown are the recoveries of Ag (NP)-binding WT vs *Rptor* Δ/+ B cells of GC-phenotype ($B220^+$ $GL7^+$ IgD^-) (c) and early memory ($B220^+$ $CD38^+$ $GL7^-$ IgD^-) (d). (e) Generation of Ag-specific IgG2c-secreting cells depends on mTORC1. Mean (±SEM) results of ELISpot assays quantitating NP-binding IgG2c (b allotype) Ab-secreting cells (ASC) from the experiments in Fig. 4c, d, and Extended Data Fig. 9b, quantified as described in Extended Data Fig. 6a.

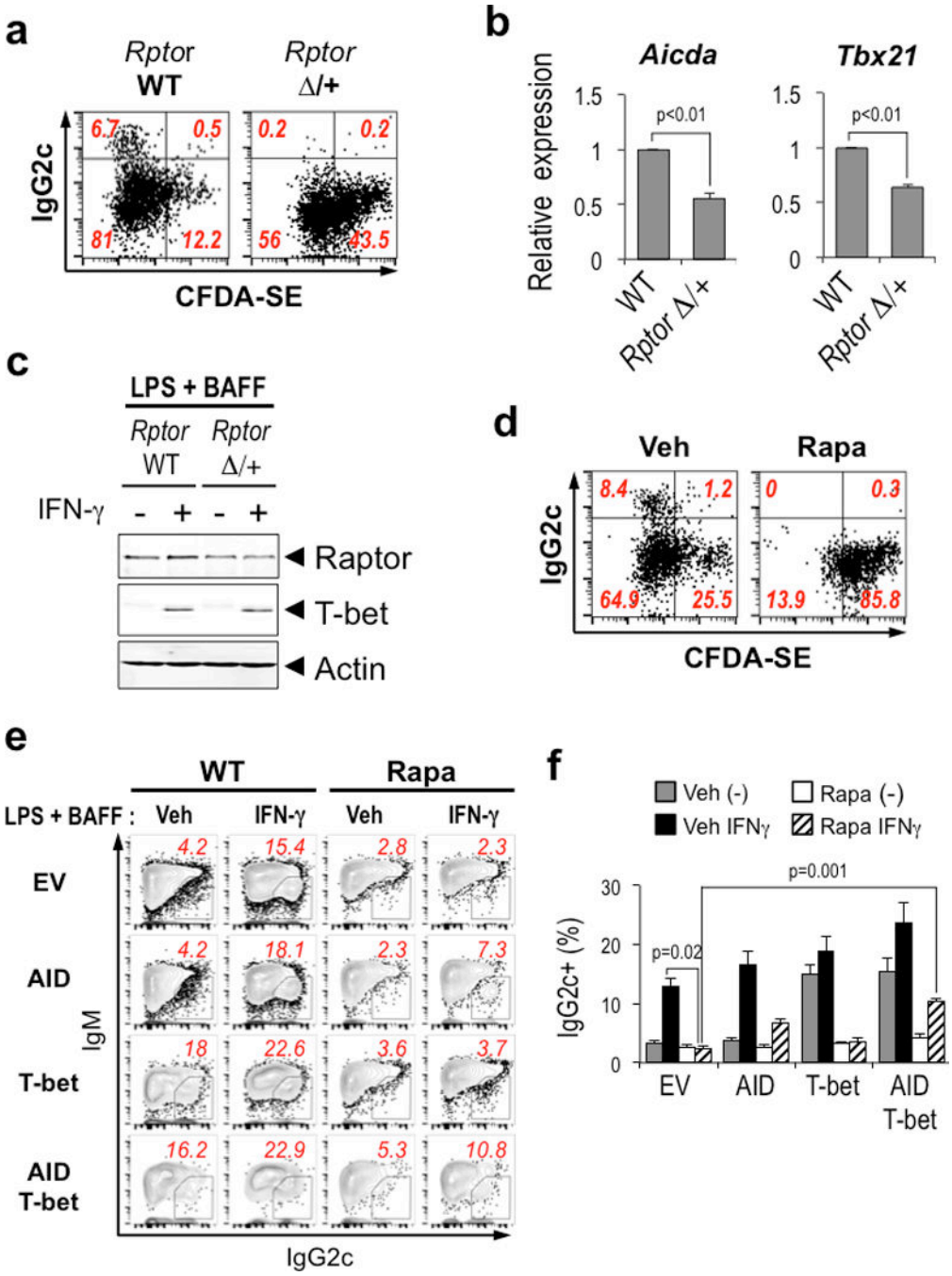

Extended Data Figure 10. mTORC1 is rate-limiting for AID expression and switching to IgG2c

(a) A division-independent mechanism dependent on mTORC1 quantity in B cell switching to IgG2c. Flow cytometric data in the B cell gate, displaying CFSE partitioning (fluorescein emission intensities) versus the IgG2c, were all from one experiment representative of three independent biological replicates. WT or *Rptor* Δ/+ B cells were stained with CFSE and cultured with LPS, BAFF and IFN-γ, and analyzed by flow cytometry. (b) WT or *Rptor* Δ/+ B cells were cultured (2 d) with LPS, BAFF, and IFN-γ. Mean (±SEM) levels of mRNA encoded by the *Aidca* (left) and *Tbx21* (right) genes measured in three independent replicate

experiments by qRT^2-PCR normalized to actin in the sample and then to the level in WT cells (set as relative level of 1). (c) Immunoblots probed for Raptor, T-bet, and actin, as indicated, using B cells as in (b). [representative of n=3 independent experiments] (d) mTOR promotes switching to IgG by division- independent mechanisms. As in panel a, but CFSE-stained WT B cells were activated and cultured for 4 days with LPS, BAFF and IFN-γ in the presence or absence of rapamycin vs vehicle. (e, f) mTORC1 regulation of AID level in collaboration with T-bet determines efficient switching to IgG2c. B cells were transduced with MIT, MIG, MIT-T-bet or pMx-GFP-AID retrovectors, and cultured with BAFF and LPS ± IFN-γ in the presence or absence of rapamycin (5 nM). (e) Representative flow data, from one experiment among three independent replicates, derived as in Extended Data Fig. 4e. (f) Mean (±SEM) frequencies of surface IgG2c$^+$ events among B220$^+$ cells analyzed 4 d after transduction are shown (n=3 independent experiments).

Supplementary Material

Refer to Web version on PubMed Central for supplementary material.

Acknowledgments

Research funding via National Institutes of Health grants R01 AI113292, HL106812 to M.B., CA164605 to S.H.; Veterans Affairs Merit award I01 BX002348 to V.H., along with support of K.S. by American Cancer Society postdoctoral fellowship PF-13-303-01-DMC, and T.C.B. by T32 DK007563 are gratefully acknowledged, as are O. Davidoff and Q. Liu for expert help with mouse management and with hypoxia chamber usage, respectively, K. Rathmell for critically reading and suggesting manuscript text, P. Young for use of an additional hypoxia chamber, H. Simkins and T. Laufer for guidance on making NP-conjugated fluors, N. Papavasiliou for the AID retrovector, C. Koch for hypoxia detection reagents, and scholarships via the Cancer Center Support Grant (CA068485) and Diabetes Research Center (DK0205930) to help pay for Vanderbilt University cores.

References

1. Victora GD, Nussenzweig MC. Germinal centers. Annu Rev Immunol. 2012; 30:429–457. [PubMed: 22224772]
2. Shlomchik MJ, Weisel F. Germinal center selection and the development of memory B and plasma cells. Immunol Rev. 2012; 247:52–63. [PubMed: 22500831]
3. Xu Z, Zan H, Pone EJ, Mai T, Casali P. Immunoglobulin class-switch DNA recombination: induction, targeting and beyond. Nat Rev Immunol. 2012; 12:517–531. [PubMed: 22728528]
4. Stavnezer J, Guikema JE, Schrader CE. Mechanism and regulation of class switch recombination. Annu Rev Immunol. 2008; 26:261–292. [PubMed: 18370922]
5. Cui G, et al. IL-7-Induced Glycerol Transport and TAG Synthesis Promotes Memory CD8+ T Cell Longevity. Cell. 2015; 161:750–761. [PubMed: 25957683]
6. Munn DH, et al. Prevention of allogeneic fetal rejection by tryptophan catabolism. Science. 1998; 281:1191–1193. [PubMed: 9712583]
7. Kaelin WG Jr. The von Hippel-Lindau tumour suppressor protein: O2 sensing and cancer. Nat Rev Cancer. 2008; 8:865–873. [PubMed: 18923434]
8. Pearce EL, Poffenberger MC, Chang CH, Jones RG. Fueling immunity: insights into metabolism and lymphocyte function. Science. 2013; 342:1242454. [PubMed: 24115444]
9. Spencer JA, et al. Direct measurement of local oxygen concentration in the bone marrow of live animals. Nature. 2014; 508:269–273. [PubMed: 24590072]
10. Patten DA, et al. Hypoxia-inducible factor-1 activation in nonhypoxic conditions: the essential role of mitochondrial-derived reactive oxygen species. Mol Biol Cell. 2010; 21:3247–3257. [PubMed: 20660157]

11. Koch CJ. Importance of antibody concentration in the assessment of cellular hypoxia by flow cytometry: EF5 and pimonidazole. Radiat Res. 2008; 169:677–688. [PubMed: 18494550]
12. Colgan SP, Taylor CT. Hypoxia: an alarm signal during intestinal inflammation. Nat Rev Gastroenterol Hepatol. 2010; 7:281–287. [PubMed: 20368740]
13. Rush JS, Liu M, Odegard VH, Unniraman S, Schatz DG. Expression of activation-induced cytidine deaminase is regulated by cell division, providing a mechanistic basis for division-linked class switch recombination. Proc Natl Acad Sci U S A. 2005; 102:13242–13247. [PubMed: 16141332]
14. Peng SL, Szabo SJ, Glimcher LH. T-bet regulates IgG class switching and pathogenic autoantibody production. Proc Natl Acad Sci U S A. 2002; 99:5545–5550. [PubMed: 11960012]
15. Kaelin WG Jr, Ratcliffe PJ. Oxygen sensing by metazoans: the central role of the HIF hydroxylase pathway. Mol Cell. 2008; 30:393–402. [PubMed: 18498744]
16. Bannard O, et al. Germinal center centroblasts transition to a centrocyte phenotype according to a timed program and depend on the dark zone for effective selection. Immunity. 2013; 39:912–924. [PubMed: 24184055]
17. Wouters BG, Koritzinsky M. Hypoxia signalling through mTOR and the unfolded protein response in cancer. Nat Rev Cancer. 2008; 8:851–864. [PubMed: 18846101]
18. Krymskaya VP, et al. mTOR is required for pulmonary arterial vascular smooth muscle cell proliferation under chronic hypoxia. FASEB J. 2011; 25:1922–1933. [PubMed: 21368105]
19. Keating R, et al. The kinase mTOR modulates the antibody response to provide cross-protective immunity to lethal infection with influenza virus. Nat Immunol. 2013; 14:1266–1276. [PubMed: 24141387]
20. Zhang S, et al. B cell-specific deficiencies in mTOR limit humoral immune responses. J Immunol. 2013; 191:1692–1703. [PubMed: 23858034]
21. Laplante M, Sabatini DM. mTOR signaling in growth control and disease. Cell. 2012; 149:274–293. [PubMed: 22500797]
22. Nimmerjahn F, Ravetch JV. Divergent immunoglobulin g subclass activity through selective Fc receptor binding. Science. 2005; 310:1510–1512. [PubMed: 16322460]
23. O'Keeffe S, et al. Immunoglobulin G subclasses and spirometry in patients with chronic obstructive pulmonary disease. Eur Respir J. 1991; 4:932–936. [PubMed: 1783083]
24. Gabrilovich DI, et al. Production of vascular endothelial growth factor by human tumors inhibits the functional maturation of dendritic cells. Nat Med. 1996; 2:1096–1103. [PubMed: 8837607]
25. Hatfield SM, et al. Immunological mechanisms of the antitumor effects of supplemental oxygenation. Sci Transl Med. 2015; 7 277ra230.
26. Konisti S, Kiriakidis S, Paleolog EM. Hypoxia--a key regulator of angiogenesis and inflammation in rheumatoid arthritis. Nat Rev Rheumatol. 2012; 8:153–162. [PubMed: 22293762]
27. Eltzschig HK, Carmeliet P. Hypoxia and inflammation. N Engl J Med. 2011; 364:656–665. [PubMed: 21323543]
28. Karhausen J, et al. Epithelial hypoxia-inducible factor-1 is protective in murine experimental colitis. J Clin Invest. 2004; 114:1098–1106. [PubMed: 15489957]

References

29. Liu Q, Davidoff O, Niss K, Haase VH. Hypoxia-inducible factor regulates hepcidin via erythropoietin-induced erythropoiesis. J Clin Invest. 2012; 122:4635–4644. [PubMed: 23114598]
30. Guertin DA, et al. Ablation in mice of the mTORC components raptor, rictor, or mLST8 reveals that mTORC2 is required for signaling to Akt-FOXO and PKCalpha, but not S6K1. Dev Cell. 2006; 11:859–871. [PubMed: 17141160]
31. Woods ML, Koch CJ, Lord EM. Detection of individual hypoxic cells in multicellular spheroids by flow cytometry using the 2-nitroimidazole, EF5, and monoclonal antibodies. Int J Radiat Oncol Biol Phys. 1996; 34:93–101. [PubMed: 12118570]
32. Cho SH, et al. Glycolytic rate and lymphomagenesis depend on PARP14, an ADP ribosyltransferase of the B aggressive lymphoma (BAL) family. Proc Natl Acad Sci U S A. 2011; 108:15972–15977. [PubMed: 21911376]

33. Cho SH, et al. B cell-intrinsic and -extrinsic regulation of antibody responses by PARP14, an intracellular (ADP-ribosyl)transferase. J Immunol. 2013; 191:3169–3178. [PubMed: 23956424]
34. Trapnell C, et al. Differential gene and transcript expression analysis of RNA-seq experiments with TopHat and Cufflinks. Nat Protoc. 2012; 7:562–578. [PubMed: 22383036]
35. Eustace A, et al. A 26-gene hypoxia signature predicts benefit from hypoxia-modifying therapy in laryngeal cancer but not bladder cancer. Clin Cancer Res. 2013; 19:4879–4888. [PubMed: 23820108]

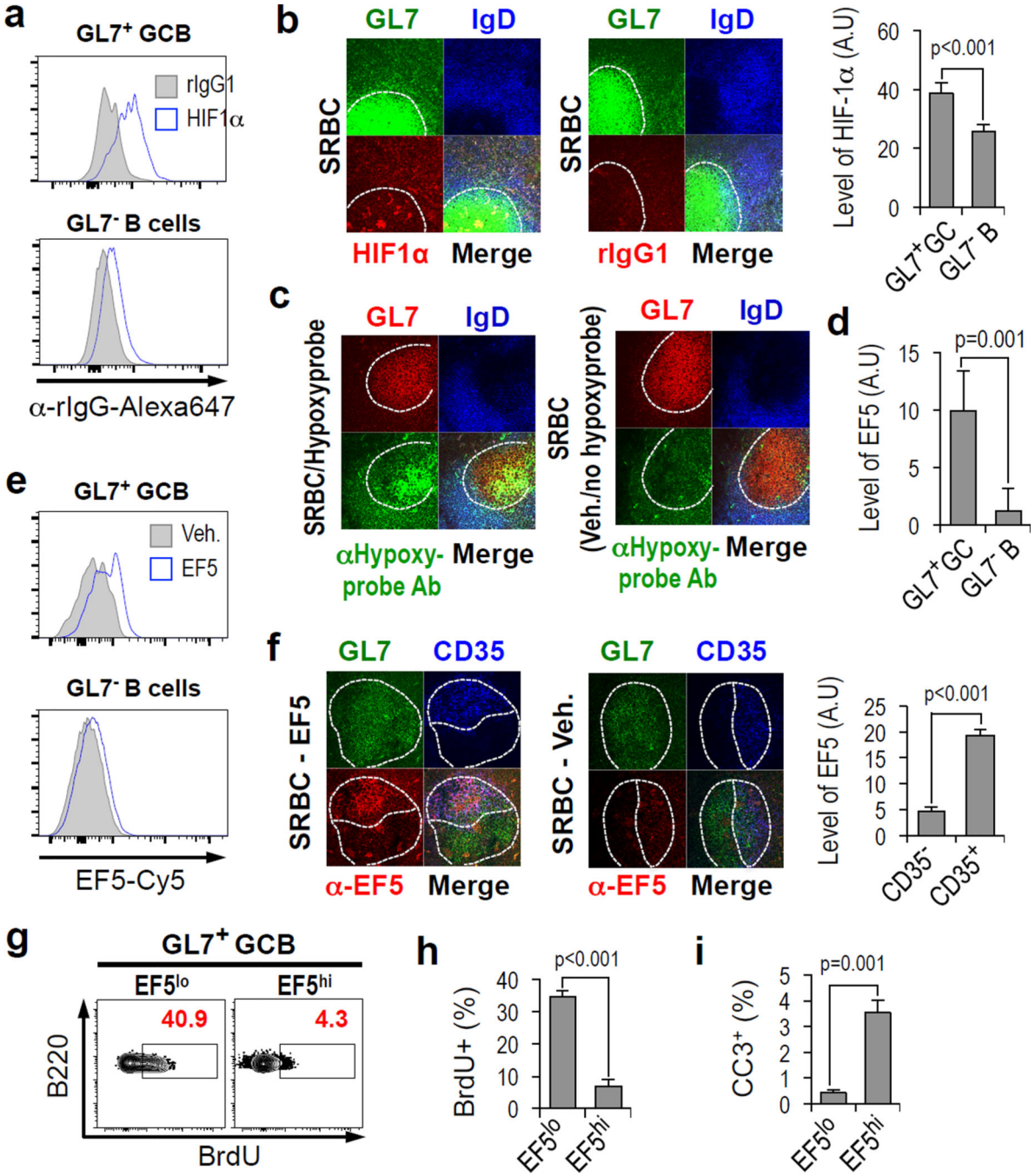

Figure 1. Hypoxia in GC Light Zones

(a) Flow cytometry of HIF-1α in GC-phenotype B cells ($GL7^+$ $B220^+$ gate) from SRBC-immunized mice, and in the $GL7^-$ $B220^+$ gate, compared to controls [rIgG1 instead of primary anti-HIF Ab; Extended Data Fig. 1a, *Hif1a* Δ B cells stained with anti-HIF-1α]. (b) Immune fluorescent staining of HIF-1α (left) or controls (right) (as in Fig. 1a) in GC ($GL7^+$ IgD^-) and surrounding follicles (IgD^+ $GL7^-$), and mean (±SEM) quantified HIF-1α signals within GCs compared to the $GL7^-$ follicular cells. Extended Data Fig. 1b, *Hif1a* Δ B cells stained with anti-HIF-1α. (c–e) GC hypoxia. Adducts, IgD, and GL7 were stained after

immunized mice were injected with EF5, pimonidazole, or PBS. (c) Anti-pimonidazole staining of spleen sections [representative of 24 GC in 9 sections from 3 independent experiments, quantified in Extended Data Fig. 1c]. (d) Bar graphs with mean (±SEM) quantified EF5 signals (Extended Data Fig. 1d) within GC compared to the $GL7^{-}$ follicles, as in Fig. 1b. (m= 19 GC from n= 5 mice each condition, PBS and EF5; x=3 independent experiments). (e) A representative flow cytometry result (n = 3 experiments) with anti-EF5 staining of spleen cells after intravital injection with EF5 or PBS, as in (c, d), gated as in (a). (f) Hypoxia maps mostly to the light zone. Spleen sections as in (e), stained for CD35, GL7, and EF5, and mean (±SEM) anti-EF5 in $CD35^{+}$ and CD35- regions, quantified as in Fig. 1d. (g) Flow cytometric measurements of S-phase ($BrdU^{+}$) GC B cells that were either hypoxic ($EF5^{hi}$) or not ($EF5^{lo}$), from mice as in (e) after BrdU injection. (h) Mean (±SEM) data for n= 7 samples in two independent experiments. (i) Mean (±SEM) fractions of cleaved caspase 3-positive ($CC3^{+}$) GCB cells gated as in (g), but stained for activated caspase 3.

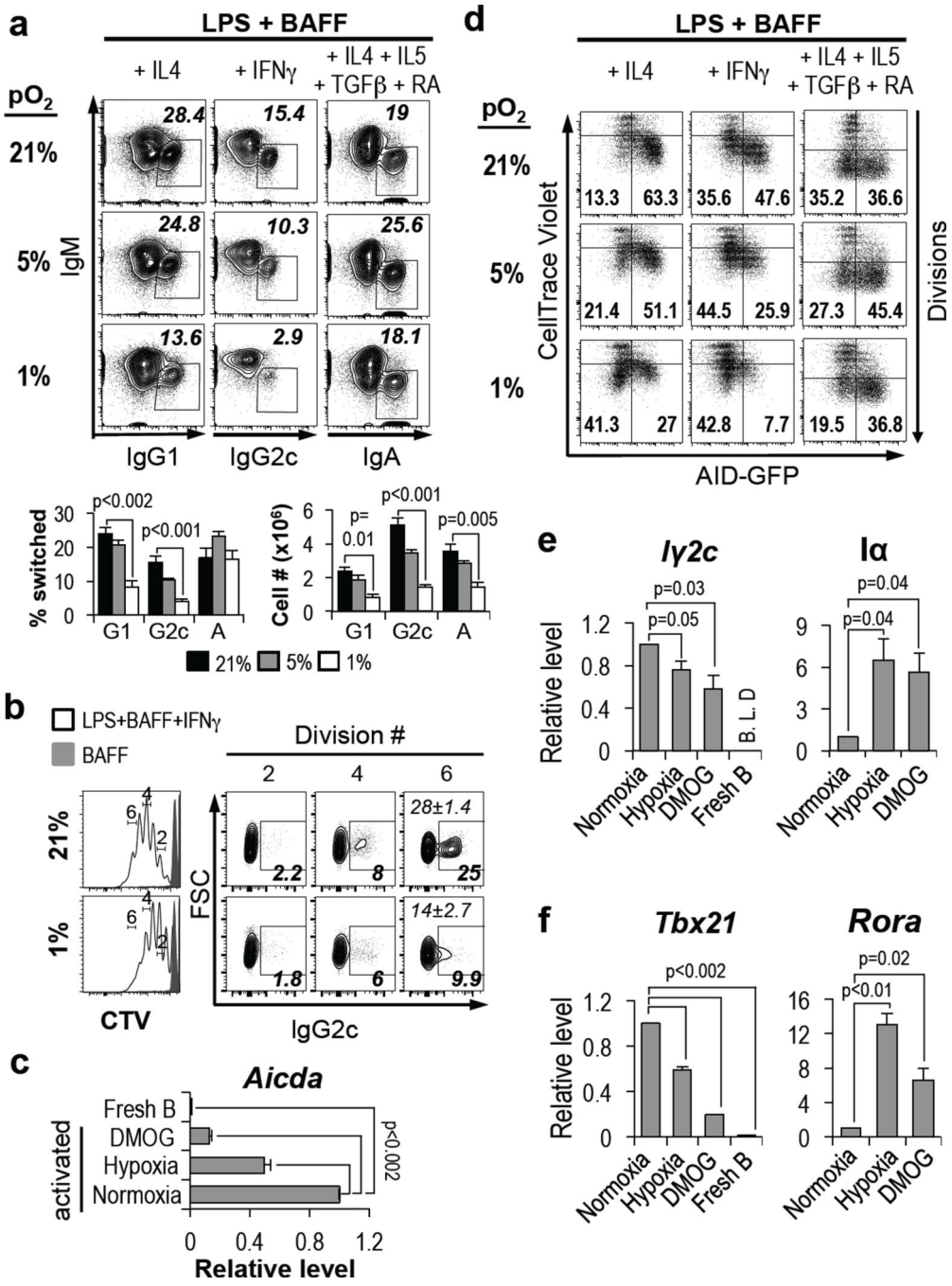

Figure 2. Hypoxia regulates B cell survival, proliferation, and class switching

(a) O_2 modulates the spectrum of Ab isotypes. Surface IgG1, IgG2c and IgA on $B220^+$-gated cells, measured by flow cytometry after activation of purified B cells culture at pO_2 of 21% ("normoxia"), 5%, or 1% ("hypoxia") using conditions promoting IgG1, IgG2c, or IgA. Flow cytometry data from one representative experiment along with bar graphs showing aggregate results of cell numbers and switch efficiencies (n=4 for 5%, n=7 for 1, 21% pO_2). (b) Flow cytometry of surface IgG2c (right panels) on B cells gated by division number (left panels) after activation of CellTrace Violet (CTV)-stained B cells and culture with IFN-γ as

in (a). Inset numbers (bold font) denote the % of switched B cells at indicated division numbers in this analysis; mean (±SEM) values from the independent replicate experiments (n=3) are *italicized*. Shaded overlay: CTV fluorescence of undivided cells cultured only in BAFF. (c, d) AID regulated by oxygen sufficiency. (c) *Aicda* mRNA was quantitated in B cells activated and cultured as in (a), or in the presence or absence of PHD inhibitor DMOG. (d) Relative AID expression, measured as GFP fluorescence in AID-GFP transgenic B cells stained with CellTrace Violet, activated and cultured in the conditions of (a, b)]. Representative GFP fluorescence versus divisions for $B220^+$ cells [mean (±SEM) quantified data from four independent replicate analyses are in Extended Data Fig. 2g]. (e, f) Hypoxia and PHD inhibition reduce T-bet and Iγ2c germ line transcript (GLT) induction, but not *Rora* or Iα. Iγ2c (e) and *Tbx21* (f) mRNA measured after B cell cultures in IgG2c conditions; Iα GLT (e) and *Rora* (f) mRNA in B cells cultured for IgA switching [B.L.D., below limit of detection]. (e, f) mean (±SEM) data (n=3–4 expts).

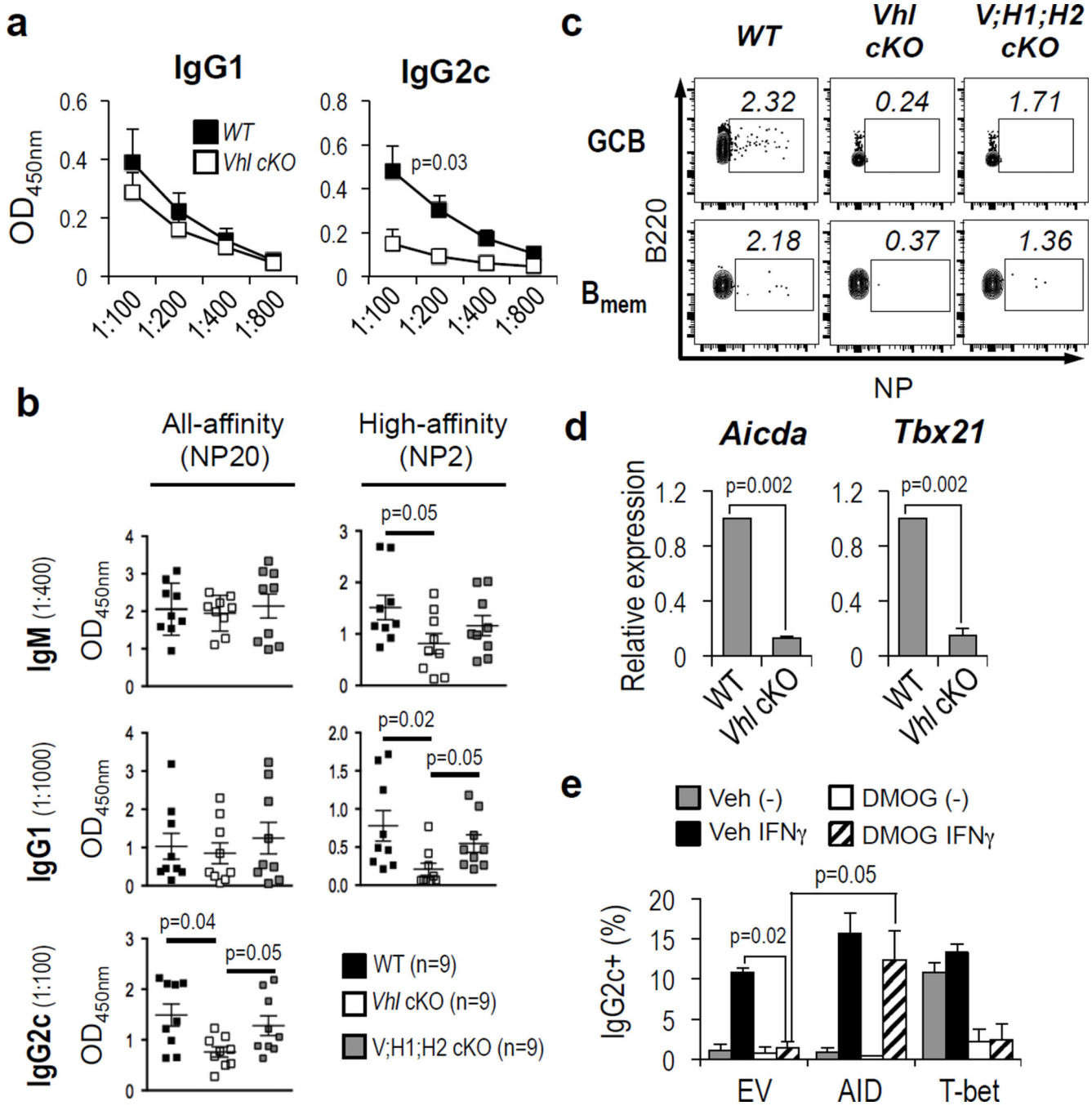

Figure 3. B cell-intrinsic role of pVHL in Ab response qualities

(a–c) In adoptive transfer experiments [schematic diagram, Extended Data Fig. 5a], B cells purified from tamoxifen-treated mice were transferred into recipients after mixing with $CD4^+$ T cells (polyclonal : Ag-specific = 4:1). Recipients were analyzed after primary (1^0) immunization or, for memory responses [Extended Data Fig. 5d], after the 1^0 and a recall immunization. (a, b) VHL reduction causes HIF-dependent alterations in Ab responses. (a) Primary NP-specific IgG2c Ab response in *Rag*^{0} recipients of WT or *Vhl* $^{f/f}$, $CreER^{T2}$ B cells from tamoxifen-treated donor mice. (n=5 recipients of each genotype, distributed

evenly between two independent replicate experiments. Other Ab isotypes are in Extended Data Fig. 5. (b) High- (NP2), or all-affinity (NP20) anti-NP Ab of the indicated isotypes in sera from immunized recipients, measured by ELISA. Each dot represents one mouse (n=9 of each genotype [WT, *Vhl* Δ/Δ (Vhl cKO), or *Vhl* Δ/Δ *Hif1a* Δ/Δ *Epas1* Δ/Δ (V;H1;H2 cKO)], distributed evenly among 3 independent experiments); horizontal lines denote the mean values. (c) HIF-dependent reduction of Ag-specific B cell populations. Flow cytometry results scoring NP-binding B cells of GC ($B220^+$ $GL7^+$ IgD^-) and early memory ($B220^+$ $CD38^+$ IgM^+ $GL7^-$ IgD^-) phenotypes. One representative result from the same mice and experiments as (b). [Extended Data Fig. 6c, d, mean (±SEM) values]. (d) VHL in B cells promotes *Aicda* and *Tbx21* expression. WT and *Vhl* Δ/Δ B cells were activated, cultured, and analyzed as in Fig. 2c. (e) B cells transduced with MIT, MIG, MIT-T-bet or pMx-GFP-AID retrovectors were cultured with BAFF and LPS ± IFN-γ in the presence or absence of DMOG. Mean (±SEM) frequencies of surface $IgG2c^+$ events among $B220^+$ cells analyzed 4 d after transduction, with flow data from one experiment in Extended Data Fig. 4e (n=3 independent experiments).

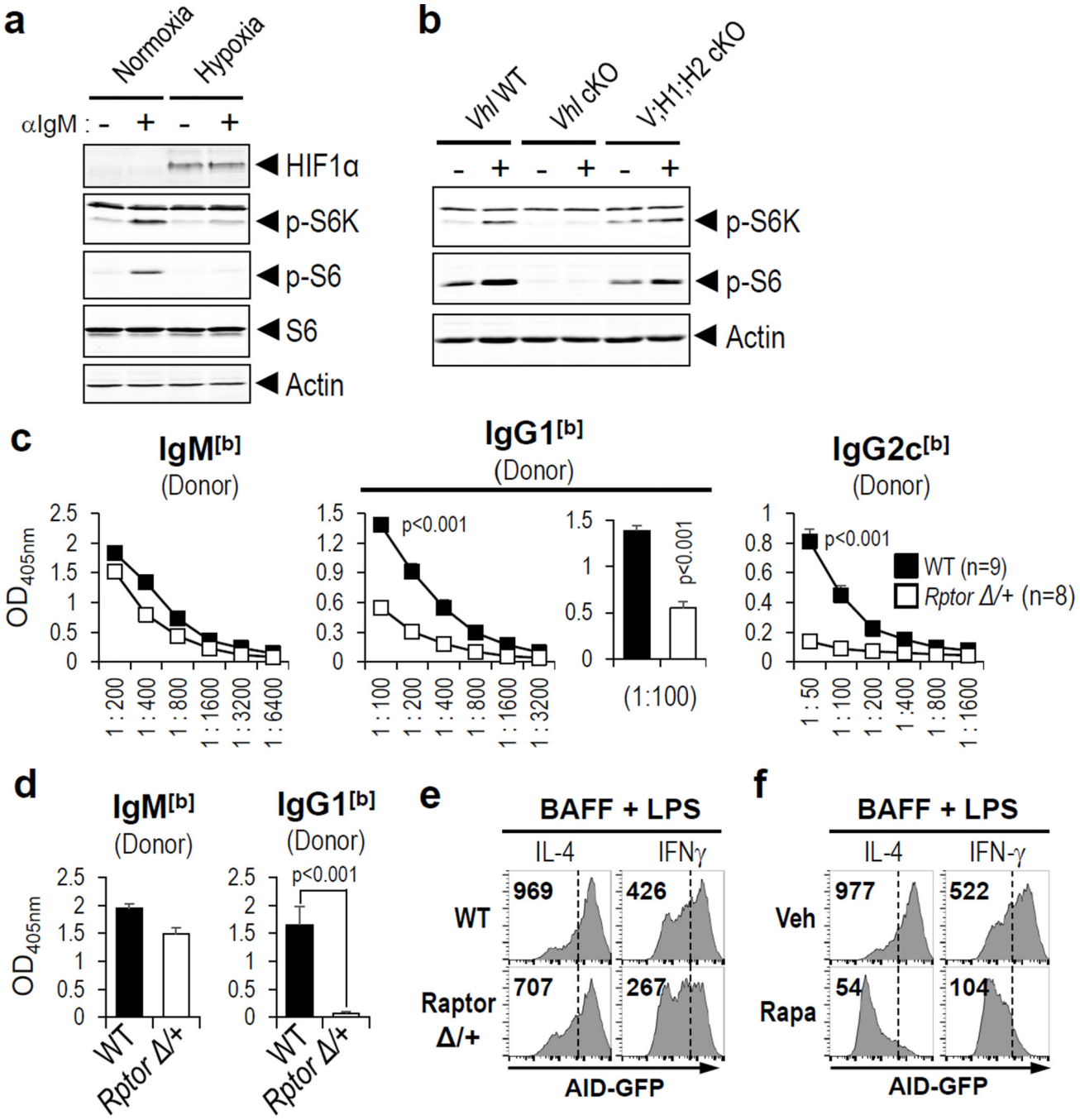

Figure 4. mTORC1 activity in B cells regulates Ab qualities but is attenuated by hypoxia

(a) Immunoblots of lysates prepared from activated B cells cultured overnight at 21% or 1% pO_2, before (−) and after (+) re-stimulation with anti-IgM. (b) Immunoblots of B cell extracts as in Fig. 4a, using WT and conditionally pVHL-depleted cells with either normal (*Vhl* cKO) or deficient (V;H1;H2 cKO) HIF expression. (c, d) Raptor promotes generation of high-affinity Ab and switch to IgG. IgH^b (donor B cell-derived)-allotype anti-NP Ab were measured after immunization of (mice IgH^a allotype) that had received WT or *Rptor* +/Δ B cells transfers. Mean (± SEM) ELISA results for all-affinity anti-NP IgG in primary

response sera from recipient mice [n=9 (WT) vs. 8 (*Rptor* +/Δ)], captured on NP_{20} (c), and high-affinity Ab (IgM, 1:100; IgG1, 1:50) captured on NP_2 (d). [IgG2c was undetectable, as in (c)]. (e, f) mTORC1 promotes AID expression. GFP in $B220^+$-gated cells in flow cytometry after B cells were cultured (4 d) with LPS, BAFF, and IL-4 or IFN-γ as indicated. (e) *Rptor* +/+ or Δ/+ AID-GFP transgenic mice. (f) *Rptor* +/+ AID-GFP cells cultured in rapamycin (10 nM) or vehicle.